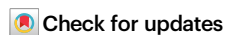


Evidence for ecological tuning of anuran biofluorescent signals

Received: 7 August 2023

Accepted: 2 October 2024

Published online: 15 October 2024



Courtney Whitcher¹✉, Santiago R. Ron², Fernando Ayala-Varela², Andrew J. Crawford³, Valia Herrera-Alva⁴, Ernesto Fernando Castillo-Urbina⁴, Felipe Grazziotin⁵, Randi M. Bowman¹, Alan R. Lemmon⁶ & Emily Moriarty Lemmon¹

Although biologists have described biofluorescence in a diversity of taxa, there have been few systematic efforts to document the extent of biofluorescence within a taxonomic group or investigate its general significance. Through a field survey across South America, we discover and document patterns of biofluorescence in tropical amphibians. We more than triple the number of anuran species that have been tested for this trait. We find evidence for ecological tuning (i.e., the specific adaptation of a signal to the environment in which it is received) of the biofluorescent signals. For 56.58% of species tested, the fluorescence excitation peak matches the wavelengths most abundant at twilight, the light environment in which most frogs are active. Additionally, biofluorescence emission spans both wavelengths of low availability in twilight and the peak sensitivity of green-sensitive rods in the anuran eye, likely increasing contrast of this signal for a conspecific receiver. We propose an expanded key for testing the ecological significance of biofluorescence in future studies, providing potential explanations for the other half of fluorescent signals not originally meeting formerly proposed criteria. With evidence of tuning to the ecology and sensory systems of frogs, our results suggest frog biofluorescence is likely functioning in anuran communication.

Biofluorescence—an organism’s ability to absorb light and re-emit it at a longer wavelength (i.e., a biological organism’s ability to fluoresce¹)—occurs in a range of taxa, including insects, plants, fishes, and reptiles² but was only recently discovered in amphibians³. Across the tree of life, fluorescence acts as a signal of sexual attractiveness in birds⁴ and spiders⁵ and correlates with organism condition in plants^{6–9} and mammals⁸. Additionally, it is hypothesized to signal resource attractiveness of flowers to bees¹⁰, to contribute to species recognition in copepods¹¹, and to facilitate camouflage in reef fishes¹². Amphibian biofluorescence has been identified in multiple anuran families, but

reports are taxonomically sparse, with descriptions of fluorescence in only a handful of species^{13–19}. While there is speculation on the function of fluorescence in amphibians, empirical tests are lacking^{16–19}.

Biofluorescence has been proposed in amphibians to act as a visual signal to potential mates, predators, or other receivers^{16–19}. According to the sensory drive hypothesis, natural selection should favor signals that maximize the received signal relative to background noise^{20–22}. Sensory drive should lead to evolutionary coupling of sensory systems, signals, signaling behavior, and habitat choice²⁰. With regard to visual signals such as biofluorescence, the coloration of an

¹Florida State University, Department of Biological Science, Tallahassee, FL 32306, USA. ²Museo de Zoología, Pontificia Universidad Católica del Ecuador, Escuela de Ciencias Biológicas, Quito 170143, Ecuador. ³Universidad de los Andes, Department of Biological Sciences, Bogotá 111711, Colombia. ⁴Museo de Historia Natural de la Universidad Nacional Mayor de San Marcos, Departamento de Herpetología, Lima 15072, Perú. ⁵Instituto Butantan, Laboratório de Coleções Zoológicas, São Paulo 05345, Brazil. ⁶Florida State University, Department of Scientific Computing, Tallahassee, FL 32306, USA.

✉ e-mail: cwhitcher@bio.fsu.edu

organism's signal is predicted to depend on the spectrum of the ambient light in the environment²³. Unlike reflected coloration, fluorescent signals are dynamic because the chemicals that produce biofluorescence (fluorophores) manipulate the light present in the environment, absorbing light at one wavelength and re-emitting it at a longer wavelength¹. Hence, fluorescing organisms are not limited to only reflecting the color of light available in the environment. Variation in the excitation and emission colors of biofluorescence, with varying fluorophore chemical mechanisms, has evolved both across and within taxonomic groups^{2,24}. This innate multidimensionality of biofluorescence may enhance evolutionary lability of this trait, enabling fluorescent organisms to respond rapidly to selection within specific abiotic and biotic environments.

Since macroscopic biofluorescence was discovered in frogs in 2017³, new accounts have documented the trait in all three orders of amphibians¹⁸ and described emission patterns that range from body-wide^{13,14} to localized patches^{15–18}. These studies employed excitation light within the 365–460 nm range (ultraviolet, violet, or blue light), obtaining results that varied in the presence and intensity of any fluorescent signals, depending upon the light source, species, and particular study^{13–18}. Under this excitation range, species produced biofluorescent emissions in the 450–550 nm range (blue to green visual light^{13–19}). Although studies have suggested that amphibian biofluorescence could increase perception of conspecific individuals in low-light environments like the twilight period^{3,18}, these predictions have not been tested.

Four criteria have been proposed for demonstrating that biofluorescence may function in signaling²⁵. First, the fluorescent pigment will absorb the dominant wavelengths of light found in the environment. Second, the fluorescence will be viewed by the receiver against a contrasting background environment. Third, organisms viewing the fluorescence will have spectral sensitivity in the fluorescent emission range, allowing the fluorescence to be perceived. Finally, the fluorescent signals will be located on a part of the body displayed during signaling. Despite the discovery of biofluorescence in diverse species, there are only two studies that assess these four criteria (see Lim et al. 2007 in jumping spiders⁵ and Haddock and Dunn 2015 in siphonophores²⁶), neither of which was focused on an amphibian.

In this study, we have two main goals. First, we aim to survey the phylogenetic breadth of anuran biofluorescence by increasing the number and taxonomic distribution of species sampled. Second, we evaluate evidence for an association between environmental characteristics and biofluorescent emission across anurans. We test the four criteria proposed by Marshall and Johnsen (2017) for establishing the ecological significance of biofluorescence. By increasing the number of species in which the trait has been observed by more than 250%, our study provides deeper insight into the phylogenetic and functional significance of biofluorescence.

Results and discussion

Survey of biofluorescence

During ten weeks of field collections at eight localities in four South American countries, we collected spectrometer measurements of biofluorescence from representatives of one salamander family, one caecilian family, and 13 anuran families (Fig. 1). We increased the percentage of anuran families tested for biofluorescence from <17% to 24%, adding 39 genera and 152 species and increasing the percentage of genera and species tested from 5% to >8% and from 0.55% to 1.99%, respectively (Supplementary Data Table 1). We more than tripled the number of species tested for this trait compared to those tested within the previous five years. We tested 528 individuals, quantifying biofluorescent emission in response to five different excitation light sources: UV – Ultraviolet (360–380 nm), VI – Violet (400–415 nm), RB – Royal blue (440–460 nm), CY – Cyan (490–515 nm), and GR – Green (510–540 nm). Prior work tested responses to only one or two of these light sources (ref. 13–18; Supplementary Data Table 1).

Fluorescence was ubiquitous; we recorded at least a low-level fluorescent signal from every individual we tested. The additional, untested light sources frequently excited biofluorescent patterns that were missed in previous studies because they used excitation wavelengths that did not closely enough match the excitation spectra of the

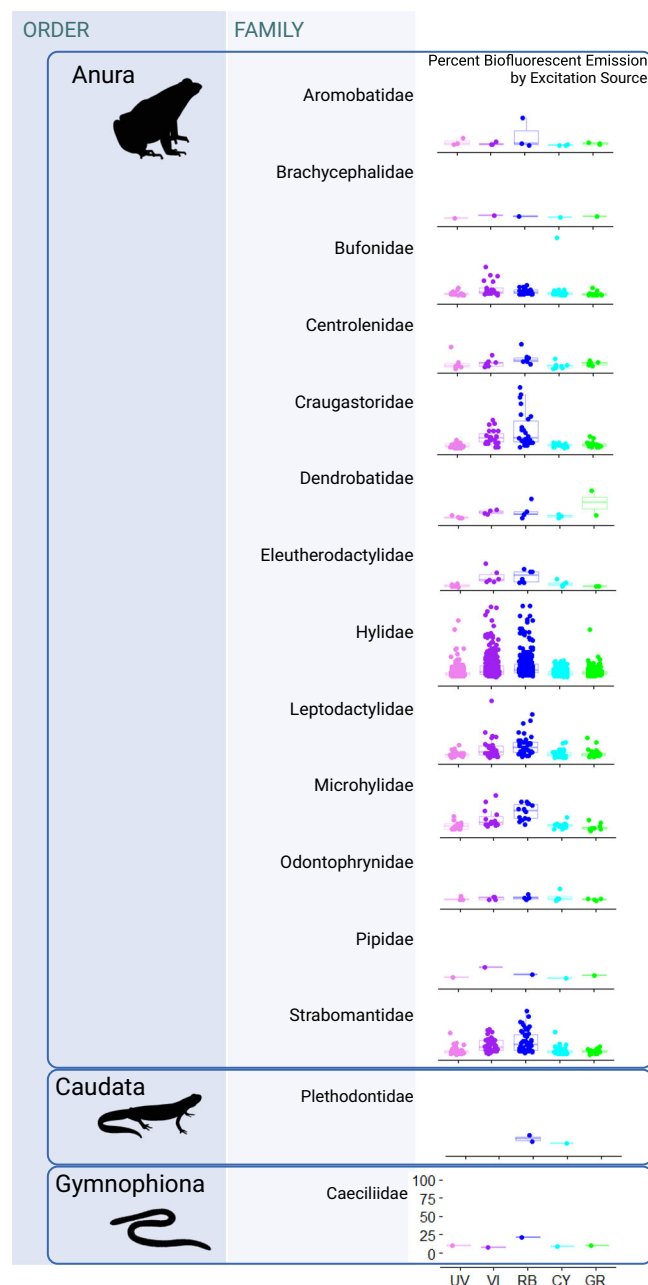


Fig. 1 | Biofluorescent emission by taxonomic family. A summary of the percent biofluorescent emission by family and excitation source. The set of box plots for each family presents the percent biofluorescent emission under the corresponding excitation light source: UV – Ultraviolet (360–380 nm), VI – Violet (400–415 nm), RB – Royal blue (440–460 nm), CY – Cyan (490–515 nm), and GR – Green (510–540 nm). The centre of each boxplot represents the median of the data. The bounds of the box represent the “interquartile range” (IQR), and the whiskers represent the minimum and maximum values of the data set. Axis labels on the bottom panel hold for each set of box plots above. Each point on the plots represents one individual (the maximum percent biofluorescent emission recorded for that individual under that excitation light source). Each individual was measured under each light source. Created in BioRender. Whitcher, C. (2023) BioRender.com/v49t214. Supplementary Data Table 4 contains the respective numeric values for these measurements.

organism's fluorescence. Additionally, low intensity fluorescent patterns may have been missed by not using a barrier filter to aid in viewing fluorescence. Without such a filter, the amount of reflected excitation light may have drowned out any biofluorescence emitted, leading to false negatives. The previously tested species in which we revealed fluorescence by utilizing an additional excitation light source include *Boana cinerascens*, *Boana lanciformis*, *Dendropsophus rhodopeplus*, *Dendropsophus sarayacuensis*, *Phyllomedusa tarsius*, and *Phyllomedusa vaillantii* (ref. 19; Supplementary Data Table 1).

Assessing variation in biofluorescence

From each of our 17,692 spectrometer recordings we calculated a maximum percent biofluorescence emission (see Methods). The maximum percentage of biofluorescent emission under each excitation light source is presented by taxonomic family in Fig. 1 (Supplementary Data Table 4) and by individual in Supplementary Data Table 5. The maximum percentage of biofluorescent emission ranged from 1.95% to 96.85% with a mean of 11.11%.

We evaluated these maximum biofluorescence recordings against the predictions for each of the four criteria proposed by Marshall and Johnsen (2017) (Fig. 2). We tested these predictions under five ecological and photoreceptor conditions: (1) Daylight irradiance and the anuran red-sensitive (RS) cone sensitivity spectra, (2) Under forest canopy irradiance and RS cone sensitivity, (3) Twilight irradiance and the anuran green-sensitive (GS) rod sensitivity spectra, (4) Full moon irradiance and GS rod sensitivity, and (5) Starlight and GS rod sensitivity. These pairings can be used to interpret how the fluorescent signal is viewed by frogs in each light environment. The results of these criterion tests for each condition are presented in Table 1, where only the blue light-induced, green fluorescent emission met all of Criteria 1–3. This match led us to focus on the blue light-induced, green fluorescent emission signal in this study. The species that meet all criteria under this condition are listed in Supplementary Data Table 2. Of the 528 individuals tested, 194 individuals from 86 species exhibited this fluorescent signal.

Just over one half (56.58%) of the anuran species tested (86 of 152 species) produced a fluorescent signal that met all of Marshall and Johnsen's proposed criteria for ecological significance (Supplementary Data Table 2) and did so under environment and visual conditions relevant and unique to frogs. Peak biofluorescent emission wavelength is shown by excitation source in Supplementary Figure S1. We found a significant difference in biofluorescent emission wavelength by excitation source ($\chi^2 = 2021.46$, $p < 2.2e-16$, $n = 2380$; Supplementary Figure S1). There were two groups of peak emission wavelengths produced by blue light excitation (440–460 nm) centered at approximately 527 nm and 608 nm. We refer to these as a “green” and “orange” peaks respectively; Supplementary Figures S1–S2. We evaluated these maximum biofluorescence emission peaks against the predictions, individually, for each of the four criteria proposed by Marshall and Johnsen below. We then expanded upon Marshall and Johnsen's original criteria by: (1) testing whether our results hold within a phylogenetic context and (2) proposing an updated key to test for ecological significance of biofluorescence that better incorporates the complexity of the previously defined criteria. We discuss how the other half of the fluorescent signals may meet the criteria for ecological significance within this expanded context.

Criterion 1: The fluorescent pigment will absorb the dominant wavelengths of the environment. We found support for this criterion under the twilight light environment: both the violet (410–415 nm) and blue (440–460 nm) excitation wavelengths matched the dominant wavelength of the twilight environment better than expected by chance ($p < 0.0001$, Table 1). Additionally, we found a significant difference in biofluorescent emission intensity by excitation source ($\chi^2 = 446.88$, $p < 2.2e-16$, $n = 2380$). Blue light excitation

(440–460 nm) produced a significantly greater percent fluorescent emission than any of the other excitation light sources (Supplementary Data Table 3; Fig. 3). The excitation wavelength that produces fluorescence is the wavelength of light absorbed by the fluorescent pigment; hence, the maximum fluorescent signal was produced by absorbing the wavelengths closest to those dominant in twilight. This pattern is consistent across anuran groups (Fig. 1) and is also maintained within a phylogenetic context, where Blue excitation (440–460 nm) produced a significantly greater percent fluorescent emission than any other excitation light source in 85.25% (Supplementary Figure S8) of the basal amphibian common ancestor trait estimates (see *Assessing Phylogenetic Structure* section).

The excitation wavelengths that produce the most fluorescence are those wavelengths most abundant at the time of day when frogs are active. In a twilight environment, wavelengths of blue light have a higher relative abundance than any other wavelengths in the environment^{27,28}. Additionally, most frogs are nocturnal and active during these twilight hours²⁹. Twilight is defined as the light environment during the time between sunset and full night when the sun is between 0° and 18° below the horizon²⁷. Illuminance values during twilight range from 10³ lux to nearly 10⁻⁴ lux, decreasing approximately a millionfold from when the sun is 10° below the horizon to when it is 15° below the horizon²⁷. These illuminance values are often the light levels which we consider “nocturnal” activity for frogs³⁰. Hence, twilight conditions are the most relevant environmental spectra in which to test the hypothesis of a function in intraspecific communication. These results are aligned with the prediction from the sensory drive model that environmental constraints will drive the evolution of a signal to match both the environmental transmission properties in the habitat and the sensory biases of the receiver in that habitat²².

Criterion 2: The fluorescence will be viewed against a contrasting background. Consistent with this prediction, the blue-light-induced fluorescent emission contrasts with the background in a twilight environment. In a twilight environment, wavelengths of blue light are at the highest relative abundance and wavelengths of orange light (~590–620 nm) are at the lowest relative abundance compared to any other wavelengths in the environment^{27,28}. The peak emission wavelengths from the frogs overlap with the wavelengths of light least dominant in the twilight environment, providing the most contrast. Both emission peaks of the blue-light-induced fluorescence match the least dominant wavelengths of the twilight environment better than expected by chance ($p < 0.0001$; Table 1). This result is consistent across both individuals and species groups. The results of the randomization test for the blue light-induced green emission individuals are presented in Fig. 4A. Additionally, to correct for unequal samples sizes across phylogenetic groups, we repeated this analysis for 10,000 subsamples of the individuals, choosing one individual from each species at random each repetition. This pattern of the blue-light-induced green fluorescence meeting Criterion 2 remains consistent for each species ($p < 0.0001$, Table 1). We also tested this pattern within a phylogenetic context, testing which models of evolution best describe the observed fluorescent emission data (see *Assessing Phylogenetic Structure* section). Hence, all fluorescent emission produced by blue light (440–460 nm), which meets Criterion 1, also meets Criterion 2 by re-emitting fluorescence at wavelengths that provide the most contrast with the background environment.

The blue light-induced fluorescent emission contrasts strongly with the background in the twilight environment. Signals should be most easily detected when they differ from the background environment³¹. Our analyses consider chromatic (hue and saturation), not achromatic (brightness), contrast. Additionally, we are working under the assumption that the background environment should proportionally reflect the wavelengths of light available in the

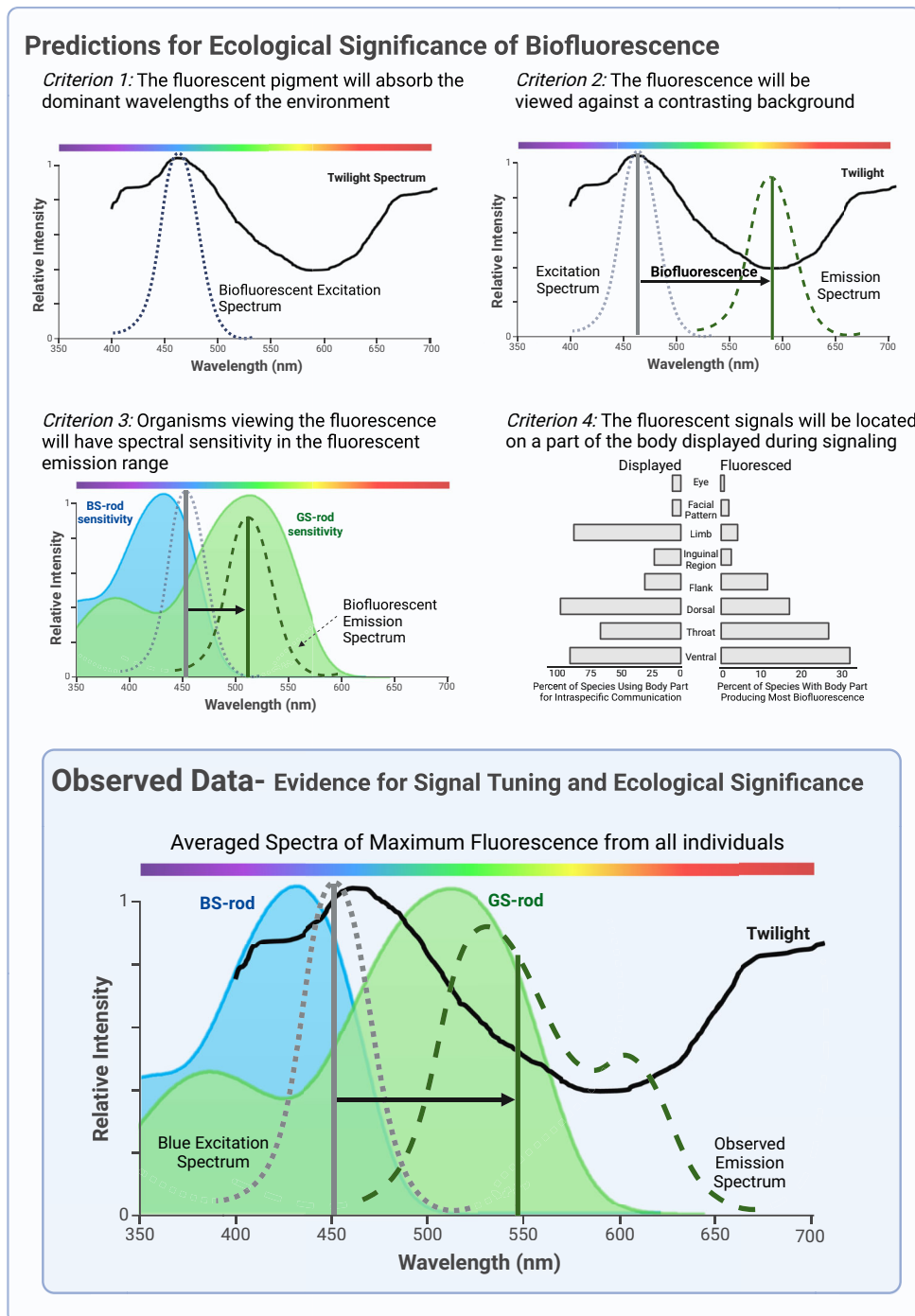


Fig. 2 | Evidence for ecological significance of biofluorescence in Anurans. The four criteria for demonstrating ecological significance of biofluorescence proposed by Marshall and Johnsen (2017), presented within the framework of a twilight environment and dim light photoreceptor visual sensitivities. The top panel presents the patterns expected when biofluorescence signals are tuned to the environment (criteria 1 and 2). Criterion 1: In a twilight environment when most frogs are active²⁹, the dominant wavelengths are ~450–460 nm (27; solid black line). The criterion predicts peak excitation (blue dotted line) of anuran fluorophores should match this wavelength range. Criterion 2: The least dominant wavelengths at twilight are ~580–610 nm (27; solid black line). The arrow represents the Stokes Shift of the biofluorescence from peak absorption wavelengths to peak re-emission wavelengths. The criterion predicts the peak biofluorescence re-emission will be centered around ~590 nm to provide the greatest contrasting background at twilight. The center panel presents the patterns expected if the biofluorescence is observable by a receiver (criteria 3 and 4). Criterion 3: Frogs have significantly more green-sensitive (peak absorption ~500 nm) than blue-sensitive rods (28; 39). Hence,

this criterion predicts peak biofluorescence re-emission will be centered around ~500 nm to match the greatest spectral sensitivity of another anuran receiver. Criterion 4: The body locations displayed during frog intraspecific communication (29–34; % of species displaying location) should match the body locations that are biofluorescent (this study; % of species for which this location produced maximum biofluorescent recording when excited by blue light, 440–460 nm). The bottom panel presents the observed data for signal tuning and ecological significance from this study. When all fluorescent spectra recorded under blue excitation light (440–460 nm) are plotted (from all body locations), they follow the general shape presented by the dashed green line. This observed fluorescent emission pattern maximizes both sensitivity of the green-sensitive rod in the anuran eye and contrast with the background environment at twilight. The results from our study show that blue-light-induced green anuran biofluorescence meets all four criteria for ecological significance. Created in BioRender. Whitcher, C. (2023) BioRender.com/t37d584.

environment, therefore these results do not take into account any fluorescence of the background environment. Nevertheless, the observed re-emission of the blue light-induced green fluorescent peak wavelengths matches the least dominant wavelengths of the twilight environment better than random (Fig. 4A). For these species, biofluorescence increases the contrast of the frog visual signal in a twilight environment, as compared to the reflected color of an individual without fluorescent properties in the same environment.

Criterion 3: Organisms viewing the fluorescence will have spectral sensitivity in the fluorescent emission range. Consistent with this criterion, the blue light-induced green fluorescent emission closely matches the spectral sensitivity of the anuran green-sensitive rod. Frogs have blue-sensitive (peak absorption ~432 nm) and green-sensitive (peak absorption ~500 nm) rods³², and there are significantly more green-sensitive rods than blue-sensitive rods in the retina of frogs³³. The emission wavelengths of the green peak overlap with the most sensitive wavelengths of light for the most abundant rod in the anuran visual system³³. The green fluorescent peak emission wavelengths match the spectral sensitivity of the green-sensitive anuran rod better than expected by chance for individuals and species ($p < 0.0001$, Table 1; Fig. 4). We then assessed which models of evolution best describe the observed fluorescent emission data (Assessing Phylogenetic Structure section). The green peak fluorescent emission produced by blue light (440–460 nm), which meets the first two criteria, also meets Criterion 3 by matching the spectral sensitivity of an anuran receiver in dim light.

Considering that both Criterion 2 and Criterion 3 must be met to interpret biofluorescence as an ecologically significant trait, we compared the blue light-induced green emission peak to a tradeoff spectrum of the wavelengths that would maximize both receiver sensitivity and background contrast simultaneously (see Methods). We divided the green-sensitive rod spectrum³⁴ by the twilight irradiance spectrum²⁷ to obtain the tradeoff spectrum. The green fluorescent peak emission wavelengths match the tradeoff spectrum better than expected by chance ($p < 0.0001$; Fig. 5). In 194 individuals spanning 86 species, anuran biofluorescence absorbs the wavelengths most dominant in the twilight environment and re-emits that light to match the tradeoff between visual sensitivity and background contrast, maximizing both. Additionally, this green emission peak produces the most intense fluorescence, re-emitting up to nearly 97% of the light shone on the frog in some cases (Supplementary Figure S2).

Thus, the most intense biofluorescent emission maximizes the conditions of Criteria 2 and 3 simultaneously. The green peak fluorescent emission produced by blue light (440–460 nm) meets the criteria for ecological significance of biofluorescence with respect to a conspecific receiver. Yovanovich and colleagues (2017) found specific amphibian color discrimination and phototaxis preference of green over blue signals only under the dim lighting conditions in which frogs are active. An individual that re-emits blue light as green, under dim-light conditions, increases its visual signal to other frog receivers. Violet-induced fluorescence contributed nearly 30% to the total emerging light under twilight conditions in *Boana punctata*³. As violet light produced the second highest biofluorescent emission in our study, only behind blue light, the contribution of blue-light-induced anuran biofluorescence in twilight conditions is likely even higher. Our evidence of a match between the anuran fluorescent signal and anuran optical sensitivity suggests biofluorescence is increasing the visual signal of frogs to conspecifics. The evidence of ecological and spectral tuning of anuran biofluorescence suggests this trait is likely functioning in communication in these species.

The individuals (~half of total) with a blue light-induced orange fluorescent peak emission wavelength, however, do not match the spectral sensitivity of the green-sensitive anuran rod better than random. This finding could suggest that orange fluorescence may be non-

adaptive or may serve as a signal to a different intended receiver (e.g., a predator or other heterospecific viewer of the signal). Here, we only evaluated the criteria for ecological significance of biofluorescence within the context of the biology and ecology of other anuran receivers, thus this work does not address the visual sensitivities of non-anuran receivers (e.g., a predator or prey viewer of the signal) or the varying environments in which these types of interspecific communications occur²⁷. Below, we expand upon Marshall and Johnsen's original criteria and propose an updated key for ecological significance of biofluorescence that we believe better incorporates the complexity of the previously defined criteria. We then evaluate these blue light-induced orange fluorescent signals and discuss how they may meet the criteria for ecological significance within this expanded context.

Criterion 4: The fluorescent signals will be located on a part of the body displayed during signaling. Consistent with this prediction, we found biofluorescence on regions of the body often displayed during intraspecific signaling, such as the dorsal surface and vocal sac, but location varied across species (Supplementary Data Table 2; see Discussion). Our literature review revealed that the mechanics of visual signaling are not known in the majority of frog species (Supplementary Data Table 2, Supplementary Data Table 5). Thus, fully assessing the behavioral function of specific fluorescent patterns must be reserved for future studies that combine descriptions of biofluorescent regions of the body with detailed ethograms of signaling patterns.

The maximum biofluorescent emission for most individuals was produced under blue (440–460 nm) excitation light (261 of 512 individuals; Fig. 6). Within this subset of individuals, 32% of the maximum biofluorescent emission recordings came from a ventral pattern, 28% from the throat, 18% from a dorsal pattern, 11% from the flank, 5% from the inguinal region, 3% from a limb, 2% from a facial pattern, and 1% from the eye (Fig. 2, Criterion 4 observed data; Supplementary Data Table 6). For this criterion, we considered the maximum fluorescent emission recording from each individual under any excitation light source, as this insured that only one body location per individual was considered (see Methods). Examining the maximum biofluorescent emission recording for each individual under each excitation light source (as in the analyses above), however, produced similar percentages of fluorescence by body location (Supplementary Data Table 7).

Within these body regions, we found great variation in the pattern of biofluorescence (Fig. 6). In some individuals, dorsal biofluorescence resulted from secretions from the frog skin (as in *Boana atlantica*), but in others it was present in distinct locations (as in *Hamptophryne boliviana* and *Scinax strigilatus*). We observed ventral biofluorescence that was widespread, condensed to specific patterns, and/or scattered in a speckled pattern (as seen in *Boana geographica*, *B. lanciformis*, and *Proceratophrys renalis*, respectively). Additionally, ventral biofluorescence often showed both green and orange emission (~527 nm and ~608 nm; as seen in *B. geographica* and *P. renalis*). Finally, we found biofluorescence present in distinct regions of the frog body of some individuals, such as the forelimbs, throat, or eyes (as seen in *Chiasmocleis bassleri*, *Scinax trapicheiroi*, and *B. calcarata* respectively).

Many of the parts of the body in which fluorescence was found are displayed during intraspecific signaling in nature (Fig. 2, Criterion 4 panel). The percentage of documented visually-communicating anuran species grouped by body region of the visual signal is shown in Fig. 2, Criterion 4. Overall, 97% of species display the dorsal, 92% ventral, 89% limb(s), 69% throat, 29% flank, 24% inguinal region, 5% eye, and 5% facial pattern (of 62 species^{35–40}); Additionally, many of these species display multiple regions of the body, potentially sending different information to different receivers (e.g., to attract females or to deter rival males^{35–40}); Three of these locations are also the most common biofluorescent areas found in species we tested (dorsal, ventral, and throat; Fig. 2; Supplementary Data Table 6), a finding that

Table 1 | Evaluation of Criteria 1–3 under each light environment and photoreceptor visual sensitivity condition

Condition (Environment and Photoreceptor)	Excitation	Emission	Meet Criterion 1 (Absorb Dominant Environment)	Meet Criterion 2 (Contrast Environment)	Meet Criterion 3 (Match Vision)
Daylight and RS Cone	UV	Blue	no	individual ($p < 0.0001$) / species ($p = 0.0112$)	individual ($p > 0.9999$) / species ($p > 0.9999$)
	VI	Green	no ($p > 0.9999$)	individual ($p = 0.9979$) / species ($p = 0.9453$)	individual ($p < 0.0001$) / species ($p = 0.0079$)
	RB	Green	no ($p > 0.9999$)	individual ($p = 0.9967$) / species ($p = 0.9669$)	individual ($p < 0.0001$) / species ($p < 0.0001$)
		Orange	no ($p > 0.9999$)	individual ($p > 0.9999$) / species ($p > 0.9999$)	individual ($p < 0.0001$) / species ($p < 0.0001$)
Under Canopy and RS Cone	UV	Blue	no	individual ($p = 0.9373$) / species ($p = 0.8852$)	individual ($p > 0.9999$) / species ($p > 0.9999$)
	VI	Green	no ($p > 0.9999$)	individual ($p = 0.6994$) / species ($p = 0.7726$)	individual ($p < 0.0001$) / species ($p = 0.0079$)
	RB	Green	no ($p = 0.996$)	individual ($p > 0.9999$) / species ($p > 0.9999$)	individual ($p < 0.0001$) / species ($p < 0.0001$)
		Orange	no ($p = 0.996$)	individual ($p > 0.9999$) / species ($p = 0.9998$)	individual ($p < 0.0001$) / species ($p < 0.0001$)
Twilight and GS Rod	UV	Blue	no	individual ($p > 0.9999$) / species ($p > 0.9999$)	individual ($p < 0.0001$) / species ($p < 0.0001$)
	VI	Green	yes ($p < 0.0001$)	individual ($p = 0.9953$) / species ($p = 0.8154$)	individual ($p < 0.0001$) / species ($p < 0.0001$)
	RB	Green	yes ($p < 0.0001$)	individual ($p < 0.0001$) / species ($p < 0.0001$)	individual ($p < 0.0001$) / species ($p < 0.0001$)
		Orange	yes ($p < 0.0001$)	individual ($p < 0.0001$) / species ($p < 0.0001$)	individual ($p > 0.9999$) / species ($p > 0.9999$)
Full Moon and GS Rod	UV	Blue	no	individual ($p < 0.0001$) / species ($p < 0.0001$)	individual ($p < 0.0001$) / species ($p < 0.0001$)
	VI	Green	no ($p > 0.9999$)	individual ($p = 0.5444$) / species ($p = 0.6849$)	individual ($p < 0.0001$) / species ($p < 0.0001$)
	RB	Green	no ($p > 0.9999$)	individual ($p > 0.9999$) / species ($p = 0.9996$)	individual ($p < 0.0001$) / species ($p < 0.0001$)
		Orange	no ($p > 0.9999$)	individual ($p > 0.9999$) / species ($p > 0.9999$)	individual ($p > 0.9999$) / species ($p > 0.9999$)
Starlight and GS Rod	UV	Blue	no	individual ($p < 0.0001$) / species ($p < 0.0001$)	individual ($p < 0.0001$) / species ($p < 0.0001$)
	VI	Green	no ($p > 0.9999$)	individual ($p < 0.0001$) / species ($p < 0.0001$)	individual ($p < 0.0001$) / species ($p < 0.0001$)
	RB	Green	no ($p > 0.9999$)	individual ($p < 0.0001$) / species ($p < 0.0001$)	individual ($p < 0.0001$) / species ($p < 0.0001$)
		Orange	no ($p > 0.9999$)	individual ($p > 0.9999$) / species ($p = 0.9760$)	individual ($p > 0.9999$) / species ($p > 0.9999$)

Bolded values indicate significance at $\alpha = 0.05$. Only blue light induced green fluorescence meets all of Criteria 1–3 ($p < 0.0001$; italicized row). Sample sizes are $n = 152$, 151, 86, and 130 for each emission type, respectively, where there are 27 overlapping species across blue-light-induced induced green and orange emission to account for multiple peaks in some fluorescent emission spectra.

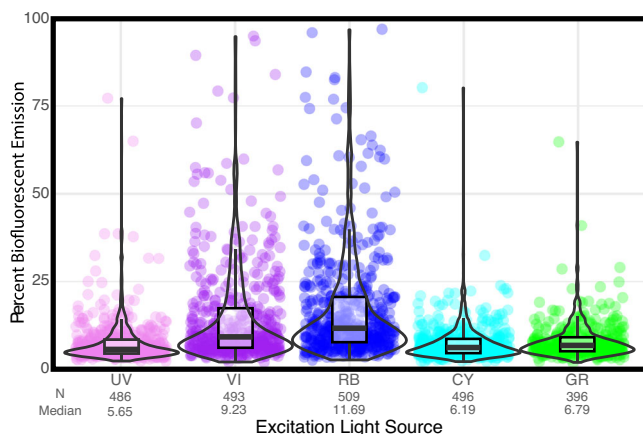


Fig. 3 | Blue light produces the most intense biofluorescence emission in Anurans. Emission intensity (percent of reflected light realized as biofluorescent emission) is shown for five excitation light sources: UV – Ultraviolet (360–380 nm), VI – Violet (400–415 nm), RB – Royal blue (440–460 nm), CY – Cyan (490–515 nm), and GR – Green (510–540 nm). Each point represents one individual (the maximum percent biofluorescent emission recorded for that individual under that excitation light source). The centre of each boxplot represents the median of the data. The bounds of the box represent the “interquartile range” (IQR), and the whiskers represent the minimum and maximum values of the data set. We utilized a non-parametric Kruskal-Wallis one-way analysis of variance test and Pairwise Dunn’s tests with Holm adjustment to determine if the wavelength of biofluorescent emission differed by excitation light source. There is a significant difference in biofluorescent emission intensity by excitation source ($\chi^2 = 446.88$, $p = 2.05e-95$, $n = 2380$) with blue light excitation (RB, 440–460 nm) producing a significantly greater percent biofluorescent emission than any of the other excitation light sources. The blue light source also has the closest excitation wavelength to the dominant wavelengths of the twilight environment (see Supplementary Figure S3).

is consistent with Criterion 4. For example, the male *Dendropsophus parviceps* individual we tested had its maximum fluorescence located on the lateral flank region and induced by blue light (96.85% emission intensity). This species is known to have multiple intraspecific visual displays, including toe trembling, arm waving, foot flagging, and throat displays³⁹. This fluorescent flank region of the body is specifically presented during the limb waving displays; hence, the green fluorescent emission of this body region is likely contributing to the visual signal of these intraspecific displays in dim light. Increased sampling within each species and further species-specific examination is needed to evaluate the contribution of fluorescence to intraspecific visual displays, since the body locations utilized in intraspecific signaling vary widely across and within anuran groups. We documented the individual body locations from which fluorescence was recorded and noted which species are lacking visual behavior information (Supplementary Data Table 2, Supplementary Data Table 5). These data highlight gaps in the literature that should be addressed next to assess significance of biofluorescence for intraspecific communication.

The fluorescent locations and patterns we observed in our study can provide some insight into potential functions of biofluorescence in anurans. For example, dorsal or facial fluorescent patterns could be employed for species recognition in certain groups (as fluorescent signals are used in stomatopods⁴¹ and proposed to be used in reef fishes¹²). In addition, fluorescent throat surfaces, which represent the brightest body region in 28% of our study individuals, could be used for mate choice or species recognition via male vocal sac expansion and contraction during calling (blue-light-induced fluorescence; Fig. 6; Supplementary Data Table 6). The role of fluorescent signals in mate choice in other taxa (specifically in budgerigar parrots⁴ and jumping spiders⁵) and recent findings of sexual dimorphism in amphibian fluorescence¹⁹ make this a likely function worthy of exploration. Fluorescence in the inguinal (inner thigh) region, normally invisible when the frog is at rest, could serve to startle a potential predator while its prey escapes⁴². Additionally, the relatively low occurrence of biofluorescence in the inguinal region could be attributed to the

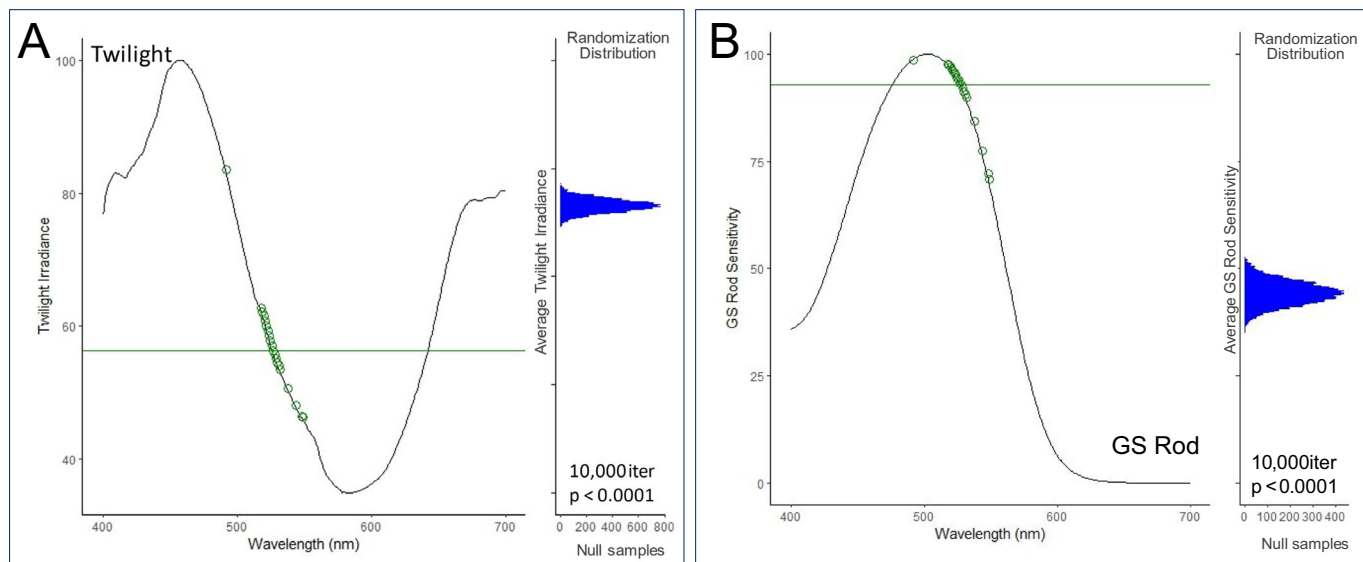


Fig. 4 | Measures of biofluorescence emission in amphibians satisfies two of Marshall and Johnsen’s criteria for ecological relevance of biofluorescence. **A** Criterion 2 (fluorescence will be viewed against a contrasting background): wavelength of peak emission in anurans (green circles) tends to be different than the most abundant wavelengths in background twilight ($p < 0.0001$; black line digitized with permission from Cronin et al., 2014). **B** Criterion 3 (organisms viewing the fluorescence will have spectral sensitivity in the fluorescent emission range): peak emission wavelengths (green circles) match peak sensitivity of anuran

green-sensitive (GS) rod of the anuran visual system better than expected by chance ($p < 0.0001$; black line obtained from³⁴). In each panel, the observed wavelength of emission for each individual frog is presented as a colored circle ($n = 194$). The mean irradiance and sensitivity values of the environment and GS rod at each emission wavelength was not directly measured in this study but obtained from irradiance/sensitivity spectra. Randomization tests were used to generate null distributions and test for significance (see text for details).

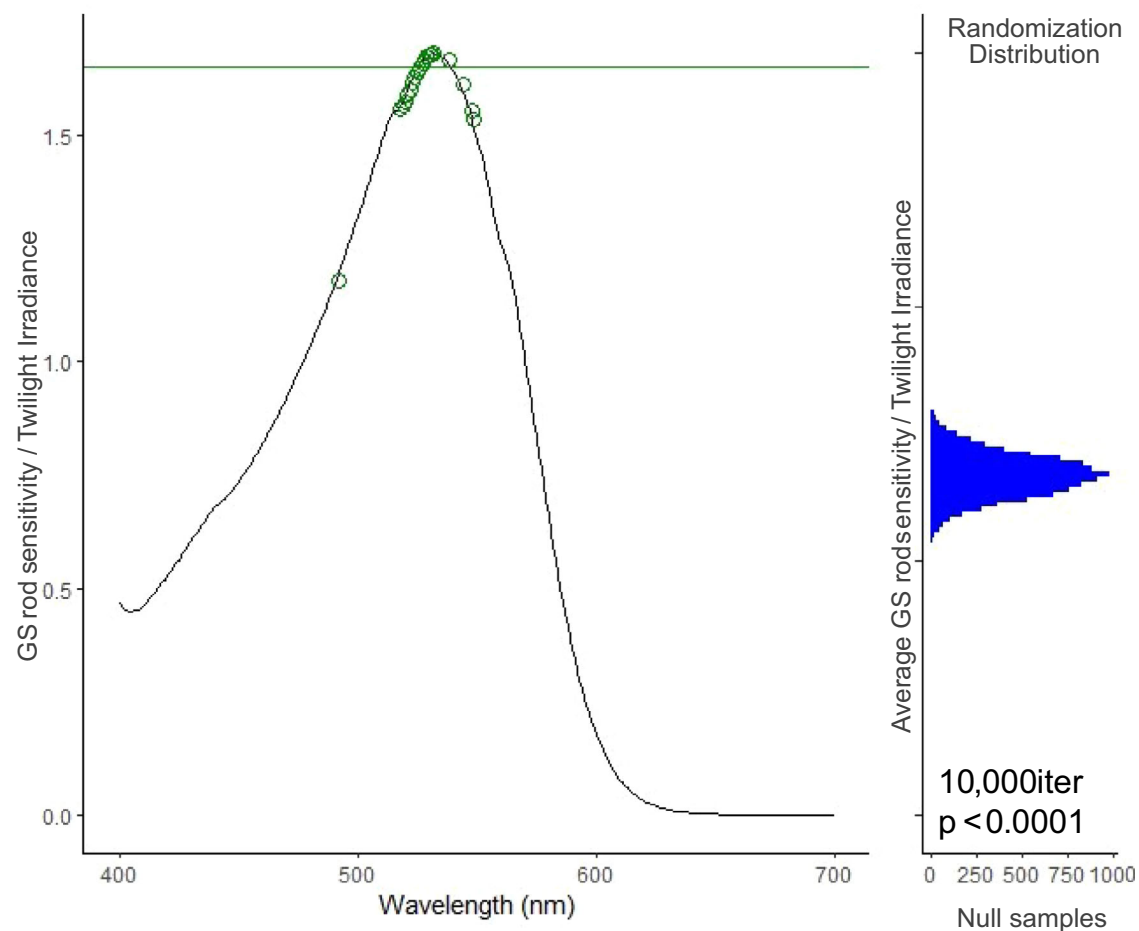


Fig. 5 | Biofluorescence increases visibility among anurans at twilight. The black line represents the tradeoff between visual sensitivity and background contrast (green-sensitive rod sensitivity curve divided by twilight irradiance curve; i.e., the spectrum that maximizes both visual sensitivity and contrast with the background environment simultaneously). The observed average tradeoff value (the observed test statistic) is presented as a horizontal line for the observed green emission peaks produced by blue (440–460 nm) excitation light ($n = 194$ colored points on graph). The null distribution of 10,000 samples is presented on the panel to the

right (blue distribution). The p-value in the bottom right-hand corner presents results of the comparison of the values in the randomization distribution to the observed test statistic. A randomization test was used to generate the null distribution and test for significance (see text for details). The green fluorescence emission peak wavelengths produced by blue excitation light match the tradeoff between the visual sensitivity of the green-sensitive anuran rod and the contrast with the twilight environment better than expected by chance ($p < 0.0001$).

possibility that these color patterns are primarily associated with anti-predator coloration serving as a form of interspecific rather than intraspecific communication. Future work should evaluate frog fluorescence signals for ecological tuning to the specific environment and vision characteristics of predator receivers to examine if these signals are visible in a predation context.

In some taxa, patterns of biofluorescence appear to be evolutionarily conserved. For example, species from two genera of microhylids have similarly fluorescent arms: *Chiasmocleis bassleri* (this study; Fig. 6) and *Gastrophryne elegans*¹⁷. In other taxa, biofluorescence trait evolution appears much more labile, as seen in the extreme variation in pattern and location within the hyliid genus *Boana*. We found that *B. atlantica* has intensely fluorescent secretions, *B. geographica* has an elaborate fluorescent dorsal pattern, *B. lanciformis* has multi-colored emission of the ventral surfaces and limbs, and *B. calcarata* has intense fluorescence of the eyes/irises (Fig. 6). As the many missing taxa are characterized with further work, a clearer picture of the evolutionary lability of biofluorescence will emerge.

Assessing phylogenetic structure

Our data span all three amphibian orders, 15 amphibian families, 41 genera, and 155 species. To assess whether phylogenetic non-

independence between measurements could affect our results, we performed several additional analyses of the criteria above, taking phylogenetic structure into account. For all phylogenetic analyses we utilized a time calibrated phylogeny obtained from Timetree.org⁴³; Supplementary Figure S6). To evaluate Criterion 1, we completed an ancestral state reconstruction for our trait measuring fluorescent intensity (the percent biofluorescent emission trait) under each excitation light source (Supplementary Figure S7). We compared the estimated percent biofluorescent emission at the basal node of the amphibian tree (Supplementary Data Table 9; Supplementary Figure S8) across these analyses. Blue excitation (440–460 nm) produced a greater percent fluorescent emission than any other excitation light source in 85.25% (Supplementary Figure S8) of the percent biofluorescent emission trait estimates for the most recent common ancestor of the amphibian clade.

To evaluate Criteria 2 and 3 within a phylogenetic context, we examined the evolution of the average blue light-induced emission wavelength for each species within the context of each of the five ecological and photoreceptor conditions. We found the wavelength of maximum vision/environment tradeoff under each condition (Supplementary Figure S9) and ran a set of analyses with constrained optima under Ornstein-Uhlenbeck evolution, where the constrained

Variation in Location of Max Fluorescence under RB excitation

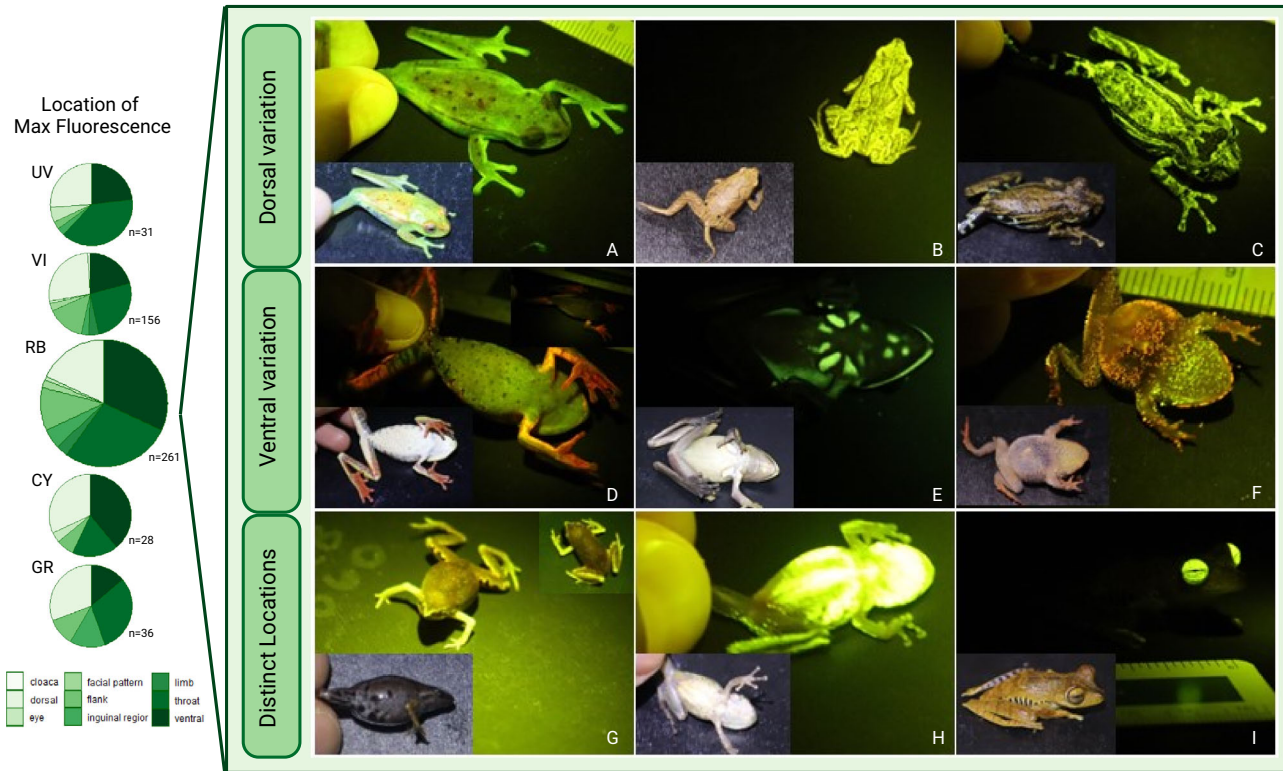


Fig. 6 | Maximum biofluorescence by body location. Pie charts (left) present the body locations from which the maximum biofluorescent emission recording was taken from each individual. Body regions are summarized into the following nine groups: cloaca, dorsal surface, eye, facial pattern, flank, inguinal region, limb, throat, and ventral surface. Photographs (right) illustrate variation in the patterns of biofluorescence produced by blue (440–460 nm) excitation light. The species photographed, in order from left to right are: (top) (A) *Boana atlantica*, (B) *Hamptophryne boliviana*, (C) *Scinax strigilatus*, (middle) (D) *Boana geographica*, (E) *Boana lanciformis*, (F) *Proceratophrys renalis*, (bottom) (G) *Chiasmocleis basleri*, (H) *Scinax trapicheiroi*, and (I) *Boana calcarata*. Each species panel includes a photograph taken under blue (440–460 nm) excitation light through a 500 nm longpass filter and a photograph of the same individual taken under a full spectrum

light source (inset). Dorsal biofluorescence was exhibited via secretions from the frog’s skin (as in *Boana atlantica*) or located in specific positions on the skin (as in *Hamptophryne boliviana* and *Scinax strigilatus*). Ventral biofluorescence was documented as widespread, condensed to specific patterns, or scattered in a speckled pattern (as seen in each individual of the middle row respectively). Additionally, ventral biofluorescence often showed both green and orange emission (~527 nm and ~608 nm; as seen in *Boana geographica* and *Proceratophrys renalis*). Finally, distinct regions of the frog body, such as the arms, throat, or eyes sometimes produced the greatest biofluorescent emission recording from an individual (as seen in each individual of the bottom row respectively). Created in BioRender. Whitcher, C. (2023) BioRender.com/b34v891.

Table 2 | Akaike’s information criterion (AIC) comparison of constrained optima Ornstein-Uhlenbeck evolution models for the evolution of blue light-induced green fluorescence

Condition	LnL	Numparams	AIC	AICc_wt	ΔAIC
Twilight and GS Rod	– 152.9	3	311.8	1.00	0.00
Starlight and GS Rod	– 158.2	3	322.5	0.0048	10.68
Full Moon and GS Rod	– 163.0	3	332.1	3.9e-05	20.28
Daylight and RS Cone	– 177.2	3	360.3	2.9e-11	48.54
Under Forest Canopy and RS Cone	– 196.2	3	398.4	1.6e-19	86.6

The constrained optima for each condition represent the peak wavelength of fluorescence from the tradeoff spectrum of that specific environmental and vision condition. The twilight and anuran green-sensitive rod condition was the best model for the evolution of the blue light-induced green fluorescent signal ($\Delta AIC < 2$, italicized).

optima correlated to the peak wavelength of fluorescence from the tradeoff spectrum of each environmental and vision condition. The models were compared with Akaike’s information criterion (AIC). The twilight and anuran green-sensitive rod condition was the best model for the evolution of the blue light-induced green fluorescent signal (Table 2).

We were only able to include a fraction of the species tested in these phylogenetic structure analyses due to limitations in the available amphibian phylogenies (84 of the 155 species were available in a time-calibrated phylogeny from Timetree.org⁴³) and due to limitations

of ancestral state reconstruction methods. Current methods of ancestral state reconstruction for continuous variables cannot handle missing data, so any species tip for which we did not have estimates had to be trimmed from the tree. Despite these drawbacks, our findings from the phylogenetically aware analyses were consistent with the uncorrected results above. Blue light-induced green fluorescence meets all criteria for ecological significance within a twilight environment and an anuran receiver context. However, the fluorescence from nearly half of our individuals remained unexplained, spurring us to

Dichotomous Key for Ecological Significance of Biofluorescence

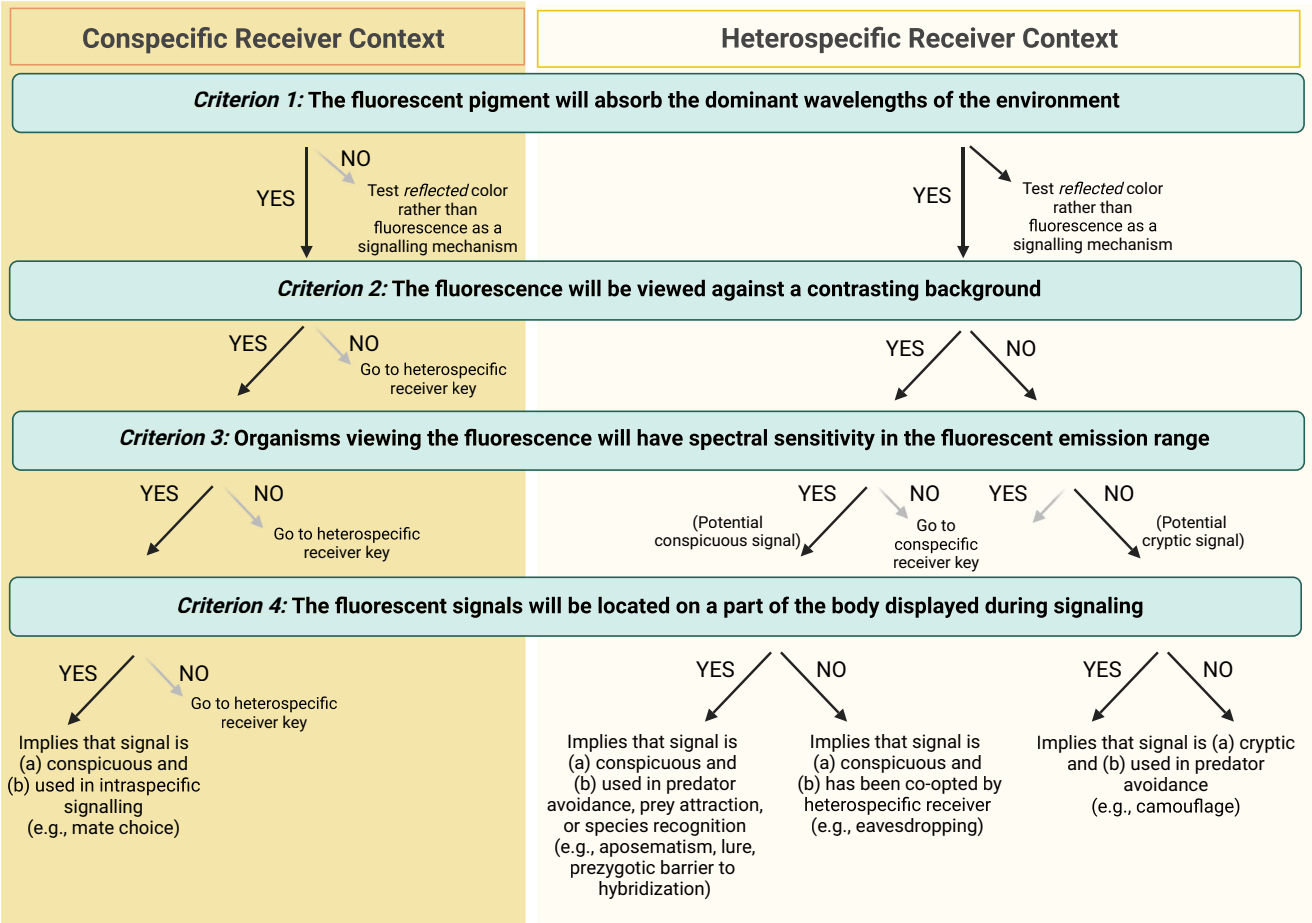


Fig. 7 | Proposed expansion of Marshall and Johnsen's criteria for ecological significance of biofluorescence. We propose the presented dichotomous key to incorporate the complexity of the previously defined criteria. Marshall and Johnsen's previous checklist for ecological significance of fluorescence is represented by the left most path of the key. Note the addition of different receiver contexts (conspecific vs. heterospecific; left vs. right panels) and the opportunity for not meeting certain criteria to be signals of cryptic coloration (via "NO" paths). Our

newly proposed key now incorporates both cryptic and conspicuous signals as ecologically significant explanations for the evolution of biofluorescence. We also propose an expansion of the term "background environment" in Criterion 2 to include both the habitat environment and the individual's skin environment as, depending on context and size/extent of biofluorescent patch, either could be the relevant background against which the signal is being viewed. Created in BioRender. Whitcher, C. (2024) BioRender.com/x53d269.

Table 3 | Akaike's information criterion (AIC) comparison of constrained optima Ornstein-Uhlenbeck evolution models for the evolution of blue light-induced orange fluorescence

Condition	LnL	Numparams	AIC	AICc_wt	ΔAIC
Anuran Green Skin Fluorescence and GS Rod	− 941.7	3	1889	0.49	0.00
Chlorophyll b Fluorescence and GS Rod	− 941.8	3	1890	0.46	0.12
Under Forest Canopy and RS Cone	− 943.9	3	1894	0.055	4.37
Daylight and RS Cone	− 948.6	3	1903	0.0005	13.78
Chlorophyll b Fluorescence and RS Rod	− 980.1	3	1966	1.1e-17	76.72
Twilight and GS Rod	− 992.4	3	1991	4.7e-23	101.4
Starlight and GS Rod	− 1002.0	3	2010	3.3e-27	120.5
Full Moon and GS Rod	− 1010.0	3	2026	1.1e-30	136.5

The constrained optima for each condition represent the peak wavelength of fluorescence from the tradeoff spectrum of that specific environmental and vision condition. Two environmental/vision conditions were equally good models for the evolution of the blue light-induced orange fluorescent signal ($\Delta AIC < 2$, *italicized*). These conditions are (1) the wavelengths that maximize contrast with the anuran green skin fluorescence background environment and maximize matching the visual sensitivity curve of the anuran Green-sensitive rod and (2) the wavelengths that maximize matching both the fluorescent chlorophyll b background environment and the Green-sensitive rod visual sensitivity curve.

examine and expand upon the current criteria for testing the ecological significance of biofluorescence.

A proposed expansion of Marshall and Johnsen's Criteria and assessment of the anuran orange fluorescent signal using an updated key for ecological significance

The individuals (-half) with a blue light-induced orange fluorescent peak emission wavelength do not meet Marshall and Johnsen's criteria for ecological significance, as currently defined. Here we outline two limitations to these criteria. First, Marshall and Johnsen listed their criteria as a checklist, where all criteria must be met with a "Yes" to support ecological significance of the biofluorescent signal. This checklist format misses several biologically relevant scenarios. For example, if fluorescence is viewed against a matching environment, instead of a contrasting one (Criterion 3), this could suggest the signal is utilized in crypsis against predators. A second and related limitation of their checklist is they do not define the context in which the fluorescent signal is ecologically significant. We addressed these two limitations in our updated key to test for the ecological significance of biofluorescence (Fig. 7). Specifically, we changed the criteria format from a checklist to a dichotomous key and provided two different contexts (a conspecific receiver context and a heterospecific receiver context) in which to evaluate the signal for ecological significance. Our proposed key now incorporates both cryptic and conspicuous signals as ecologically significant explanations for the evolution of biofluorescence.

We evaluated the blue light-induced orange fluorescent signals within a phylogenetic context for Criteria 2 and 3 (following the same methods for the evaluation of blue light-induced green fluorescence described above). In addition to the five previously defined vision/environment conditions (e.g., Red-sensitive Cone/Daylight, Green-sensitive Rod/Twilight, etc.), we assessed the evolution of the orange fluorescent trait under three more environmental conditions (Supplementary Figure S10; Table 3). The first and second conditions we added were chosen to test whether the orange fluorescence of frogs could be utilized as a cryptic signal for camouflage. The plants that comprise the background of many frog environments have chlorophyll-induced, biofluorescent signatures, with peak fluorescent excitation wavelengths of ~453 nm and peak emission wavelengths of ~644 nm⁷⁻⁹. We hypothesized that the orange fluorescent signal (average peak excitation ~440 nm and average peak emission ~618 nm) may closely match the, chlorophyll-induced, fluorescence of the plants in its habitat, allowing the frog to better blend into its background environment and avoid predation. Utilizing the fluorescent emission signal of chlorophyll b (raw spectral data obtained from photochemcad.com), we evaluated the vision/environment conditions of: (1) the wavelengths that maximize matching both the peak emission of the fluorescent chlorophyll background environment and the peak Red-sensitive cone visual sensitivity and (2) the wavelengths that maximize matching both the fluorescent chlorophyll b background environment and the Green-sensitive rod visual sensitivity (Supplementary Figure S10, panels A and B respectively). These peak wavelength values were used to set the constrained optimum parameter in the phylogenetic evolutionary models as described above and in *Methods*. While the red-sensitive cone visual sensitivity curve utilized in this analysis was obtained from frogs³⁴, many anuran predators also have red-sensitive cones. We found that the chlorophyll b and green-sensitive rod condition was one of the two best supported models for the evolution of blue light-induced orange fluorescence (Table 3). Because amphibians are the only known terrestrial vertebrates to have the dual rod system for color discrimination in dim light environments, this result could suggest that blue light-induced orange fluorescence may serve as camouflage from predation by other anurans.

The third condition we added to this analysis was one in which the background "environment" is the green biofluorescent signal of the

ventral surface of a frog's skin (Supplementary Figure S10; Table 3). This was an equally best supported model for the evolution of the orange anuran fluorescent signal (Table 3). The greatest proportion of blue light-induced orange fluorescence was located on the throat (Supplementary Data Table 10). This is contrasted with our previous finding that the greatest proportion of blue light-induced green fluorescence was located on the ventral surface (Fig. 6). Considering these patterns, we hypothesized that the orange fluorescence of the throat may be presented against a highly contrasting green background during calling/mating if an individual frog has both an orange fluorescent throat and a green fluorescent ventral body surface. We see this pattern of an orange fluorescent vocal sac against a green fluorescent ventral surface in *Osteocephalus buckleyi*, for example (Supplementary Figure S11). We calculated the maximum wavelength of the tradeoff spectrum between this green fluorescent emission spectrum and the anuran green-sensitive rod (Supplementary Figure S10) and utilized this wavelength to define the optimum in our evolution model analyses (Table 3). Again, the models of evolution that best describe the evolution of the orange fluorescent emission wavelength are: (1) the condition which maximizes matching the Chlorophyll b fluorescence environment and the anuran green-rod sensitivity and (2) the condition that maximizes both contrast with the green fluorescent anuran skin spectrum and sensitivity of the anuran green-sensitive rod ($\Delta AIC < 2$, Table 3).

Following our proposed dichotomous key for ecological significance (Fig. 7), we suggest that blue light-induced orange fluorescence may act as a cryptic camouflage signal in some individuals and a conspicuous mate choice signal in other individuals. While further exploration is needed (see *Caveats and future work* below), our study offers support for specific hypotheses of ecological significance of orange fluorescence in frogs. These two hypotheses can be used to focus future studies evaluating these fluorescent signals at the species level. As more data is collected, we suggest further reevaluation of the proposed criteria for ecological significance of biofluorescent signals.

Caveats and future work

The evidence for multiple different evolutionary forces driving the evolution of the green and orange fluorescent emission wavelengths in frogs may help explain the high rate of intraspecific polymorphism we discovered. Further work is needed to assess the consistency of biofluorescence patterns documented here across anuran groups occupying different ecological niches. For instance, members of Dendrobatidae and Pipidae appear to differ from most other taxa and not follow the pattern of peak biofluorescence being excited by blue light (440–460 nm) (although our sample sizes were too small for robust testing; Fig. 1). This inconsistency is likely due to differences in their ecology compared to most frogs. Since dendrobatids are diurnal and pipids are aquatic, their environmental spectra, transmission, and hence the resulting wavelengths available for producing a fluorescent signal differ drastically from the rest of the anuran families^{27,28}. Because these ecological differences can shape visual sensitivities⁴⁴⁻⁴⁶, they should be taken into careful consideration in future studies. In this study, we were limited to using the red-sensitive cone and green-sensitive rod spectra obtained from the red-eyed treefrog³⁴, a primarily nocturnal species. Future work should compare the maximum biofluorescent emission wavelength to species specific spectral sensitivities as these data become available.

We found that only the blue-light-induced green fluorescent emission met predictions for Criteria 1–3 (Table 1). It should be noted, however, that these methods did not include phylogenetic non-independence (only the methods described under the *Assessing Phylogenetic Structure* heading include phylogenetic non-independence) and that several other maximum emission wavelengths met both Criterion 2 and Criterion 3, including UV-induced blue fluorescence under full moon conditions, and UV, VI, and RB green fluorescence under

starlight conditions. While the excitation wavelengths do not match the dominant wavelengths of the environment in these cases, there may still be sufficient light available at these wavelengths to excite the fluorescent signal. Spectra specifying where the excitation and emission wavelengths fall with respect to each environmental irradiance and photoreceptor sensitivity spectrum can be found in the Supplementary Materials (Supplementary Figures S3–S5).

Implications

We found evidence for anuran biofluorescence across a broad phylogenetic spectrum. Just over one half (56.58%) of the frog species tested produced a fluorescent signal that met all of Marshall and Johnsen's criteria for ecological significance and did so under environment and visual conditions relevant and unique to frogs. Our study supports the idea that some anurans may be utilizing fluorescent signals as an intraspecific communication mechanism. The biofluorescence in many frog species matches the perception peak of anuran green rods but strongly differs from background colors reflected during normal frog breeding hours, making biofluorescence most visible during this time. Additionally, we proposed an expanded key for ecological significance of biofluorescence which future studies of biofluorescence can utilize. Our updated criteria framework provided potential explanations for the other half of the anuran fluorescent signals not originally meeting all criteria for ecological significance. In sum, our results suggest that sensory drive may underlie the evolution of frog biofluorescence, motivating future research on its function in anuran communication.

Methods

Collections in Ecuador were made under the authority of the *Ministerio de Ambiente, Agua y Transición Ecológica* No. 2034. Vouchers were deposited in The Zoology Museum at the Pontifical Catholic University of Ecuador (QCAZ). Collections in Peru were made under the authority of the *Ministerio de Agricultura y Riego* No. 2022-0000809. Vouchers were deposited in the *Museo de Historia Natural San Marcos (UNMSM)*. Collections in Colombia were made under the authority of the *Permiso marco* No. 1177 of 09 October 2014 granted by the *Autoridad Nacional de Licencias Ambientales (ANLA)* to the *Universidad de los Andes (UniAndes)*. Relevant animal care and use protocols for amphibians were approved by the *CICUA* of *UniAndes* under *POE 22-001* and vouchers were deposited in the *Museo de Historia Natural C.J. Markinkelle* at *UniAndes*. Collections in Brazil were made under the authority of the *Brazil Instituto Chico Mendes de Conservação da Biodiversidade (ICMBio)* No. 66597 via collaboration with the *Instituto Butantan*. FG was supported by grants from *Conselho Nacional de Desenvolvimento Científico e Tecnológico (CNPq)*, 312016/2021–2 and 405518/2021–8 and from *Fundação de Amparo à Pesquisa do Estado de São Paulo (FAPESP)*, 2016/50127–5 and 2022/12660–4. Vouchers were deposited at the *Instituto Butantan* and registered in the *Sis-Gen* system. All data collection methods were approved by the *IACUC* under protocol *IPROTO202100000007*.

Experimental design

This study was designed to discover, document, and assess variation in amphibian biofluorescence. To discover fluorescence across the diversity of amphibians, we conducted field surveys of this trait across eight sites representing much of the amphibian biodiversity of lowland South America, the region with the highest species richness of amphibians in the world. While most specimen acquisition was opportunistic via nightly trail surveys, we focused our efforts on collection of anurans, especially treefrogs from the *Hylidae* family and the *Dendropsophus* genus within this family. We made the choice to focus our sampling on *Dendropsophus* and *Hylidae* to increase our sample size for future genus- and family-specific studies, balancing the breadth and depth of our data collection. To document biofluorescence, we collected spectrometer recordings and photographs

of individual amphibian fluorescence under five excitation sources. To assess variation in the amphibian biofluorescent traits we discovered, we used analysis of variance tests. Specifically, we assessed if biofluorescent emission differed by excitation wavelength to search for evidence of ecological tuning of this recently discovered trait.

Study sites

We collected data at eight sites spanning four countries across South America. We chose study sites to maximize the diversity of hylid frogs, as preliminary work has shown that this group has the highest presence and diversity of biofluorescence found to date^{13–18}. We focused efforts on collecting individuals from the genus *Dendropsophus*; our collection sites include the geographic ranges of 77 of the 108 recognized *Dendropsophus* species. These sites include field stations in four South American countries: Colombia, Ecuador, Peru, and Brazil, including four states within Brazil (SP, ES, BA, AM). Data collection occurred from March to May of 2022, within the breeding season of most anurans at these sites. Our field collection schedule was as follows: March 2nd–10th at Yasuní Scientific Station, Ecuador; March 13th–21st at El Amargal Nature Reserve, Nuquí, Chocó, Colombia; March 24th–April 2nd at Los Amigos Conservation Hub (CIRCA), Peru; April 8th–13th sampling in Fazenda Michelin, Ubatuba, São Paulo (SP); April 17th–20th sampling in Estação Biológica Augusto Ruschi, Aracruz, Espírito Santo (ES); April 23rd–27th sampling in Reserva Michelin, Igrapiúna, Bahia (BA); May 2nd–5th sampling in Manaus, along Rio Negro via boat, State of Amazonas (AM); May 6th–13th sampling in Presidente Figueiredo, AM.

Field capture and specimen preparation

We collected individuals during night surveys on the trails surrounding each research station we visited. We captured individual amphibians by hand and placed them in a labelled Ziploc plastic bag with air, substrate, and water for transport back to the field station. Each individual was given a field number, and GPS coordinates were taken at the point of capture using a handheld Garmin GPS system. At the field station, all biofluorescent measurements were taken on the same night of capture (see methodology below). The following morning, we euthanized each individual, determined species and sex via dissection, collected tissues, and prepared samples for museum accession. Individual species IDs were determined via region-specific field guides and knowledge of local collaborators. All specimen capture and sample acquisition followed appropriate permit requirements for the specific site as specified above.

Collecting biofluorescence measurements

At the field station, and on the same night of capture, we tested each individual for fluorescence under five different excitation sources spanning a nearly 200 nm wavelength range (365–460 nm) using the Xite Fluorescent Flashlight System (*NightSea*). The five excitation wavelength ranges were as follows: UV – Ultraviolet (360–380 nm), VI – Violet (400–415 nm), RB – Royal blue (440–460 nm), CY – Cyan (490–515 nm), and GR – Green (510–540 nm). We focused on this range of wavelengths to encompass and expand upon wavelengths of biofluorescent excitation used in previous studies^{13–18} and to ensure that we did not miss any biofluorescent traits. The individual was held by hand beneath the light source, which was suspended above the organism via a *YSLIWC Gooseneck Tripod* stand maintained at the same height. We obtained biofluorescent emission spectra for each individual by utilizing a *Maya2000 Pro Series UV-VIS Portable Spectrometer* with its attached fiber optic cable held above the surface of the amphibian's skin while beneath the excitation light. This instrument provided information on the emission spectra and intensity of any biofluorescent signals from the frog (200–1000 nm) in response to each of the five excitation wavelengths. *NightSea* barrier filter glasses matching the respective excitation source were utilized to view and identify potential locations of biofluorescence to test on the body of

the amphibian. We utilized the live spectrometer recording acquisition feature of the *OceanView* computer application to determine if a specific location had a fluorescent signal (as defined by the presence of a visible peak at a longer wavelength than the excitation source). If any intensity peak was visible, or if it was questionable if a peak was visible, a spectrometer recording was taken with the probe held approximately two millimeters above that area of skin. We used a 1000 ms integration time for each spectrometer recording and took three recordings at each location (focusing on the same location with minimal movement between recordings) to have technical replicate measurements of the biofluorescent signal at that body location.

In addition, we photographed patterns of biofluorescence under each light source, as well as under a full-spectrum headlamp light source, using a Canon digital camera and Tiffen camera filters matching the respective excitation source (as specified by *NightSea*). Along with these quantitative measurements, we recorded qualitative descriptions of the color of skin and the color of fluorescence (i.e., what color the skin was in natural light, what color the fluorescent signal was, and where the fluorescent signal was present, from a human visual perspective).

Determining characteristics of biofluorescent measurements

We determined the peak excitation and emission wavelength and intensity from each spectrometer recording and utilized these intensities to calculate a maximum percent biofluorescence emission:

$$\left(\%BF = \frac{\text{intensity at peak emission } \lambda}{\text{intensity at peak excitation } \lambda} * 100 \right)$$

This provided our focal measure of intensity of fluorescence relative to the amount of reflected excitation light. All characterizations of spectrometer recordings were completed in R version 4.2.3 (R Core Team 2023). An ASCII file, containing intensity in photon counts for wavelengths ranging 200–1000 nm, of each spectrometer recording was saved via the *OceanView* application at time of acquisition and later loaded into R for analysis. Spectra were smoothed via a fifteen-point moving average filter to reduce noise in the spectrum. Utilizing the photobiology package (Aphalo 2015)⁴⁷, smoothed spectra were changed to an object of class spectra and normalized to the highest intensity (corresponding to the excitation light) using the `normalize()` function. We found peak excitation wavelengths by using the `which.max()` function and confining the parameters to only look for the maximum intensity within the wavelength range of the excitation light source. For example, finding the wavelength that corresponds to the highest intensity (photon count) within the wavelength range of 360–380 nm for UV excitation light, 400–415 nm for VI light, etc. Some of our excitation peak recordings were saturated (maximum >60,000 photon counts). If this was the case, the maximum intensity value available from the spectrometer recording (at 60,000 photons) was utilized. We expect data affected by this saturation would overestimate the intensity of the fluorescence emission recording, though this should not affect the overall significance of our findings because we estimate that saturation occurred at comparable levels across all excitation light sources. All peak emission wavelengths were found using the `get_peaks()` function from the photobiology package. As a fluorescent signal can produce multiple peaks, the `get_peaks()` function found all peaks at a wavelength greater than the longest wavelength of the excitation source (greater than 380 nm for UV, 400 nm for VI, etc.). Because fluorescence absorbs light and re-emits it at a longer wavelength, these peaks are all potential fluorescent signals under the respective excitation light. Within the `get_peaks()` function, we set the `ignore_threshold` to 0.01 to only collect peaks with a relative size greater than 1% as compared to the tallest (excitation) peak, and we set the span to 100 to define a peak as a datapoint within the wavelength sequence that had an intensity greater than those within a

50-count window on either side of the point. These parameters were chosen via trials adjusting parameters to find peaks of a subset of spectrometer recordings representing the diversity of emission spectra shapes (one emission peak close to the excitation peak, one peak far from excitation, two peaks, no peaks, etc.) and were chosen to reduce the probability that noise in the recording was defined as a peak. Additionally, to further assure that the chosen peaks were significant signals and not noise, any suspected emission peak with an intensity greater than the excitation peak was removed, as this was likely a sign of an inaccurate spectrometer recording. In these cases, and in any cases where no peaks were found, “NA” was input for the peak wavelength and intensity values. For blue-light-induced fluorescence, there were two main emission peaks (Supplementary Figure S1), so the second tallest excitation peak was also recorded to account for any individuals with a bimodal emission spectrum. The intensity at each peak emission wavelength was divided by the intensity at the peak excitation wavelength for the respective spectrometer recording to calculate the average percent intensity of fluorescence relative to the amount of reflected excitation light.

As stated, we acquired three spectrometer recordings from each body location on each individual to have technical replicate measurements of the biofluorescent signal at that body location. The calculated percentages of biofluorescence emission for these three recordings were averaged for each body location. Because our data set contained spectrometer recordings from a different number of body locations, and often different specific body regions, from each individual (due to the variation in physical biofluorescent patterns that we were attempting to capture across a wide range of species), we only used the maximum percent biofluorescence emission (from any body region, under each of the five excitation light sources) for downstream analyses. Hence, for all analyses of variance, the unit of measurement used was the maximum percent of biofluorescence emission recorded from each individual.

We also examined the body location from which the maximum biofluorescent recording from each individual was taken. For this, we used the maximum percent biofluorescence emission (from any body region, under any light source). Utilizing the maximum fluorescent emission recording for each individual insured that only one body location per individual was being considered, although, examining the maximum biofluorescent emission recording for each individual under each excitation light source (as in the analyses above) produced similar percentages of fluorescence by body location. For easier comparison, the body regions were summarized into the following nine groups: cloaca, dorsal (including spectrometer recordings with a body location specified from any dorsal pattern), eye, facial pattern (including lip, spots under the eye, snout, etc.), flank, inguinal region, limb (including forelimbs, thigh, etc.), throat (including vocal sac), and ventral (including any ventral pattern). The percentage of maximum biofluorescent recordings from each of the nine body locations were calculated for each light source.

Statistical analysis

We evaluated the maximum biofluorescence recordings against the predictions for each criterion proposed by Marshall and Johnsen (2017) for ecological significance for five different light environment irradiance spectra and two relevant photoreceptor visual sensitivity curves. The light environment irradiance spectra we utilized were digitized with permission from Cronin et al. 2014 and consisted of: Daylight, Under Forest Canopy, Twilight, Full Moon, and Starlight. The relevant anuran photoreceptor sensitivity curves we utilized were for the red-sensitive cone and the green-sensitive rod. Photoreceptor sensitivity curves were obtained from³⁴. For assessing ecological significance under environmental conditions relevant to frogs, we paired these light environments to their relevant anuran photoreceptor: the red-sensitive (RS) cone with day environments (Daylight and Under

Forest Canopy) and the green-sensitive (GS) rod with night environments (Twilight, Full Moon, and Starlight). We assessed each maximum fluorescent emission against Marshall and Johnsen's criteria, under these five conditions: (1) Daylight irradiance and the anuran RS cone sensitivity spectra, (2) Under forest canopy irradiance and RS cone sensitivity, (3) Twilight irradiance and the anuran GS rod sensitivity spectra, (4) Full moon irradiance and GS rod sensitivity, and (5) Starlight and GS rod sensitivity. Note, there were two groups of peak emission wavelengths produced by blue light excitation (440–460 nm) centered around approximately 527 nm and 608 nm (we refer to these as a “green” peak and “orange” peak respectively; Supplementary Figures S1–S2). Additionally, some individuals had both a green and orange peak in their emission spectra. Individuals were included in both the green and orange peak analyses separately if they had both peaks, regardless of which peak had a greater intensity. There were 194 individuals with a green emission peak and 363 individuals with an orange emission peak (145 individuals had only a green peak; 47 individuals had a green first peak and an orange second peak; two individuals had an orange first peak and a green second peak; 314 individuals had only an orange peak).

Note that an under forest canopy at night irradiance spectrum was not available, an environment that is likely relevant for many anuran species. In addition, due to the limitations of the irradiance spectra only having recordings for 400–700 nm, the fluorescent excitation and emission could only be evaluated for those recordings within this range. For example, UV excitation could not be statistically evaluated in respect to Criterion 1. However, the relative amount of ultraviolet light at ground level is estimated to be only 4%, in comparison to 44% visible light due to the blocking of UV wavelengths by the atmosphere⁴⁸, so we estimated that these UV wavelengths would not be dominant in the daytime environments (Table 1). Additionally, the emission of cyan and green-light-induced fluorescence spanned beyond 700 nm and often into the infrared range (Supplementary Figure S1). While likely not relevant to anuran sensory biology, we suggest this unique fluorescent pattern is explored further in respect to potential predators with infrared detection capabilities (such as snakes). We also completed randomization tests for Criteria 1–3 (as described below) under each light environment and photoreceptor visual sensitivity condition for diurnal individuals in daytime conditions. The results of our tests are presented in Supplementary Data Table 8, but the extremely limited samples sizes should be noted. We caution any strong interpretations from these results and suggest future studies should explore these correlations further with increased sampling.

Evaluate Criterion 1: The fluorescent pigment will absorb the dominant wavelengths of the environment. To evaluate evidence for Criterion 1, we utilized a randomization test to assess if each range of excitation wavelengths matched the most dominant wavelengths of the environment better than expected by chance. For each set of excitation wavelengths (VI 400–415 nm and RB 440–460 nm), we determined the average value of irradiance at those excitation wavelengths. This is the test statistic. We then took a sample of the same size ($n = 15$ and $n = 20$ respectively) and randomly selected a wavelength between 400 and 700 nm, then calculated a new average value of twilight irradiance for those wavelengths. We repeated this for 10,000 iterations and compared the values in the randomization distribution to the observed test statistic value to determine whether the peak fluorescent excitation matched the wavelengths most abundant in the environment better than by chance ($\alpha = 0.05$). We were only able to complete these calculations for the VI and RB excitation sources due to the limited wavelength range of our environment irradiance spectra.

Evaluate Criterion 2: The fluorescence will be viewed against a contrasting background. To evaluate evidence for Criterion 2, we assessed whether the peak emission wavelength of the blue-light-induced

fluorescence matched the least dominant wavelengths of the twilight environment better than expected by chance. Fluorescent emission wavelengths that match the least dominant wavelengths of light at twilight will produce the most contrast with the background environment.

We utilized a non-parametric Kruskal-Wallis one-way analysis of variance test and Pairwise Dunn's tests with Holm adjustment to determine if the wavelength of biofluorescent emission differed by excitation light source. As above we utilized a randomization test to assess if the emission wavelengths of each excitation source matched the least dominant wavelengths of the environment better than expected by chance. For each set of emission wavelengths within the wavelength range of our irradiance spectra (UV, VI, RB green, and RB orange), we determined the average value of irradiance at those emission wavelengths. This is the test statistic. We then took a sample of the same size ($n = 486, 493, 194$, and 363 for each emission type respectively, where there are 49 overlapping individuals between blue induced green and orange emission when accounting for multiple peaks) and randomly selected a wavelength between 400 and 700 nm, then calculated a new average value of twilight irradiance for those wavelengths. We repeated this for 10,000 iterations and compared the values in the randomization distribution to the observed test statistic value to determine if the peak fluorescent emission matched the wavelengths least abundant in the environment better than by chance ($\alpha = 0.05$).

Additionally, to correct for unequal samples sizes across phylogenetic groups, we repeated this analysis for 10,000 subsamples of the individuals. For each subsample, we choose one individual from each species at random and repeated the test statistic and null calculations as above, with samples sizes of $n = 152, 151, 86$, and 130 for each emission type respectively. There are 27 overlapping species between blue induced green and orange emission when accounting for multiple peaks. We compared the values in the randomization distribution to the observed test statistic value to determine if the peak fluorescent emission matched the wavelengths least abundant in the environment better than by chance ($\alpha = 0.05$).

Evaluate Criterion 3: Organisms viewing the fluorescence will have spectral sensitivity in the fluorescent emission range. To evaluate evidence for Criterion 3, we assessed if the peak emission wavelength of the blue-light-induced fluorescence matched the peak sensitivity of the green sensitive anuran rod better than expected by chance. As above, we utilized randomization tests with 10,000 iterations each, for both individuals and species, to determine if the fluorescent emission wavelengths under each light source match the anuran photoreceptor sensitivity curve better than expected by chance ($\alpha = 0.05$). We repeated with for both the red-sensitive cone and green-sensitive rod sensitivity curves (obtained from³⁴).

Considering that meeting both Criterion 2 and Criterion 3 is necessary to support ecological significance, we also compared the blue-light-induced green emission peak to the tradeoff spectrum of twilight irradiance and anuran rod sensitivity, as follows. We divided the green-sensitive rod spectrum³⁴ by the twilight irradiance spectrum²⁷ to obtain the tradeoff spectrum. This is the spectrum of wavelengths that would maximize both receiver sensitivity and background contrast simultaneously. Both the twilight and rod spectra were standardized before this calculation. As above, we then utilized a randomization test to assess if the green emission peak matched the tradeoff spectrum better than expected by chance. We calculated the average tradeoff value at the emission wavelengths of the green peak. This is the test statistic. We then took a sample of the same size (194 individuals) and randomly selected a wavelength between 400 and 700 nm, then calculated the tradeoff value for those wavelengths. We repeated this for 10,000 iterations and compared the values in the randomization distribution to the

observed test statistic to determine if the green peak fluorescent emission maximized the wavelengths to meet both Criterion 2 and Criterion 3 better than by chance.

Assessing phylogenetic structure

To assess whether phylogenetic non-independence between measurements affected our results, we performed several additional tests of the criteria above after accounting for phylogenetic structure. For all phylogenetic analyses we utilized a time calibrated phylogeny obtained from Timetree.org⁴³. A list of all species in the analysis was uploaded to Timetree.org, using the “Load a List of Species” option under the “Build a Timetree” function. Three species tips were not available, but inferred from Timetree, based on the same positioning on the tree. These species were *Dendropsophus hadaddi* inferred from *D. brevipollicatus*, *Physalaemus atlanticus* inferred from *P. ephippifer*, and *Diaporus gularis* inferred from *D. diastema*. We removed species tips for which we did not have data for a given analysis because the programs we used could not handle missing data for continuous trait evolution models.

To evaluate Criterion 1 within a phylogenetic context, we completed an ancestral state reconstruction for the trait of percent biofluorescent emission under each excitation light source. The percent biofluorescent emission was averaged for each species (Supplementary Data Table 11). We utilized the `anc.Bayes` function in `phytools` (⁴⁹, implemented in R v4.2.3.) to estimate the percent biofluorescent emission at the basal node of the amphibian tree for each excitation source. This value was estimated in 1000 mcmc generations and compared across excitation sources.

To evaluate Criteria 2 and 3 within a phylogenetic context, we examined the evolution of the average blue light-induced emission wavelength for each species within the context of each of the five ecological and photoreceptor conditions. The wavelength of biofluorescent emission was averaged for each species. Averages were calculated on the lists of individuals with peak blue light-induced green fluorescence (any peak, first or second) and blue light-induced orange fluorescence (any peak, first or second) from the previous criteria analyses, separately. See Supplementary Data Table 2 and Supplementary Data Table 10 for emission wavelengths averaged and samples sizes of each species. We found the wavelength of maximum vision/environment tradeoff under each of the five vision/environment conditions. Utilizing RevBayes constrained optima Ornstein-Uhlenbeck evolution models⁵⁰, we ran five analyses for each fluorescent emission dataset where the constrained optimum correlated to the peak wavelength of fluorescence from the tradeoff spectrum of each environment/vision condition. This was done by constraining the `moveAppend(theta)` parameter weight to 0.01 and constraining the `theta` prior parameter to 0.01 nm on either side of the peak tradeoff wavelength for each condition as follows. The bounds of the uniform prior for the Daylight/RSCone condition were set at (575.99, 576.01); (591.99, 592.01) for the UnderCanopy/RSCone condition; (512.99, 513.01) for the Twilight/GSRod condition; (496.99, 497.01) for the FullMoon/GSRod condition; and (503.99, 504.01) for the Starlight/GSRod condition (Supplementary Figure S9). We ran each model for 100,000 iterations (burnin generations = 20000, tuningInterval = 100). The average likelihood value from all 100,000 generations of each model was compared using Akaike’s information criterion (AIC). Models with a delta AIC value less than two were considered to fit the data equally well.

The analyses were run as above for the blue light-induced oranges fluorescence with a few additions. Three additional conditions were tested in the constrained optima modelling analyses as defined previously (see *Assessing Phylogenetic Structure in Results and Discussion*). The bounds of the uniform `theta` prior for these three conditions were defined as (617.99, 618.01) for the Chlorophyll/GSRod condition; (699.99, 700.01) for the Chlorophyll/RSCone condition; and (616.99,

617.01) for the AnuraGreenFluorescence/GSRod condition (Supplementary Figure S10). Note that unlike all other condition tradeoff spectra, the maximum wavelength for both chlorophyll conditions were calculated by taking the fluorescent chlorophyll b fluorescent spectrum divided by the photoreceptor visual sensitivity curve. This is because these conditions were chosen to test whether the orange fluorescence of frogs could be utilized as a cryptic signal for camouflage. Hence, we wanted to find the wavelengths that maximize matching both the peak emission of the fluorescent chlorophyll background environment and the peak Red-sensitive cone visual sensitivity (in contrast to finding the wavelengths that maximize peak visual sensitivity while also maximizing contrast with the background environment, as defined in Marshall and Johnsen’s original Criterion 2 and 3). Finally, the emission spectra utilized for the green anuran fluorescent signal in the final condition tested (Supplementary Figure S10, panel C), was taken from an individual of the species *Osteocephalus buckleyi* (Field number ECM 20505). For this individual *Osteocephalus buckleyi* we have both an orange fluorescent throat and a green fluorescent flank spectrometer recording under Blue (440–460 nm) excitation light. As both the flank and ventral surface of this species is mottled, we believe that the fluorescent recording from the flank is a good approximation for the fluorescence of the ventral skin surface. These spectrometer recordings are presented in Supplementary Figure S11.

Reporting summary

Further information on research design is available in the Nature Portfolio Reporting Summary linked to this article.

Data availability

All specimen data can be accessed via the museum/institution in which the individual was accessioned (ECM 20001-20528, see Methods section above). All spectrometer recordings and photographs are available by contacting the corresponding author; these raw data files available under restricted access due to vastness (>17,000 spectrometer recordings and >24,000 photographs). All other data are available in the main text or the supplementary materials. Source data are provided with this paper.

Code availability

All code is available on Dryad (Supplementary Code 1; <https://datadryad.org>, <https://doi.org/10.5061/dryad.djh9w0w5g>). <https://doi.org/10.5061/dryad.wpzgmsbxz>

References

- Johnsen, S. *The optics of life: a biologist’s guide to light in nature*. (Princeton University Press, Princeton, NJ, 2012).
- Lagorio, M. G., Cordon, G. B. & Iriel, A. Reviewing the relevance of fluorescence in biological systems. *Photochem. Photobiol. Sci.* **14**, 1538–1559 (2015).
- Taboada, C. et al. Naturally occurring fluorescence in frogs. *Proc. Natl. Acad. Sci. USA* **114**, 3672–3677 (2017).
- Arnold, K. E., Owens, I. P. F. & Marshall, N. J. Fluorescent signaling in parrots. *Science* **295**, 92–92 (2002).
- Lim, M. L. M., Land, M. F. & Li, D. Sex-specific UV and fluorescence signals in jumping spiders. *Science* **315**, 481–481 (2007).
- Lichtenthaler, H. K. & Rinderle, U. The role of chlorophyll fluorescence in the detection of stress conditions in plants. *C. R. C. Crit. Rev. Anal. Chem.* **19**, S29–S85 (1988).
- Lang, M., Stober, F. & Lichtenthaler, H. K. Fluorescence emission spectra of plant leaves and plant constituents. *Radiat. Environ. Biophys.* **30**, 333–347 (1991).
- Jung, T., Bader, N. & Grune, T. Lipofuscin: formation, distribution, and metabolic consequences. *Ann. N. Y. Acad. Sci.* **1119**, 97–111 (2007).

9. Thorp, R. W., Briggs, D. L., Estes, J. R. & Erickson, E. H. Nectar fluorescence under ultraviolet irradiation. *Science* **189**, 476–478 (1975).
10. Nemésio, A. Fluorescent colors in orchid bees (Hymenoptera: Apidae). *Neotrop. entomol* **34**, 933–936 (2005).
11. Shagin, D. A. et al. GFP-like proteins as ubiquitous metazoan superfamily: evolution of functional features and structural complexity. *Mol. Biol. Evol.* **21**, 841–850 (2004).
12. Michiels, N. K. et al. Red fluorescence in reef fish: A novel signalling mechanism? *BMC Ecol.* **8**, 16 (2008).
13. Taboada, C., Brunetti, A. E., Alexandre, C., Lagorio, M. G. & Faivovich, J. Fluorescent Frogs: A Herpetological Perspective. *South Am. J. Herpetol.* **12**, 1–13 (2017).
14. Deschepper, P., Jonckheere, B. & Matthys, J. A Light in the Dark: The Discovery of Another Fluorescent Frog in the Costa Rican Rainforests. *Wilderness Environ. Med.* **29**, 421–422 (2018).
15. Gray, R. J. Biofluorescent lateral patterning on the mossy bushfrog (*Philautus macroscelis*): the first report of biofluorescence in a rhacophorid frog, 3.
16. Thompson, M. E., Saporito, R.A., RuizValderrama, D.H., Medina-Rangel, G. F. & Donnelly, M. A. A field-based survey of fluorescence in tropical tree frogs using an LED UV-B flashlight. *Herpetology Notes*. **12**, 987–990 (2019).
17. Whitcher, C. New accounts of biofluorescence in several anuran genera (Hylidae, Microhylidae, Ranidae, Leptodactylidae) with comments on intraspecific variation. *Herpetology Notes*. **13**, 443–447 (2020).
18. Lamb, J. Y. & Davis, M. P. Salamanders and other amphibians are aglow with biofluorescence. *Sci. Rep.* **10**, 2821 (2020).
19. Cox, J. L. & Fitzpatrick, B. M. Biofluorescent sexual dimorphism revealed in a southern Appalachian endemic salamander, *Plethodon metcalfei*. *Sci. Rep.* **13**, 3588 (2023).
20. Endler, J. A. Signals, signal conditions, and the direction of evolution. *Am. Naturalist* **139**, S125–S153 (1992).
21. Bruce, M. J., Herberstein, M. E. & Elgar, M. A. Signalling conflict between prey and predator attraction: signal conflict in spiders. *J. Evolut. Biol.* **14**, 786–794 (2008).
22. Cummings, M. E. & Endler, J. A. 25 Years of sensory drive: the evidence and its watery bias. *Curr. Zool.* **64**, 471–484 (2018).
23. Cole, G. L. & Endler, J. A. Male courtship decisions are influenced by light environment and female receptivity. *Proc. R. Soc. B.* **283**, 20160861 (2016).
24. Gruber, D. F. et al. Adaptive evolution of eel fluorescent proteins from fatty acid binding proteins produces bright fluorescence in the marine environment. *PLoS ONE* **10**, e0140972 (2015).
25. Marshall, J. & Johnsen, S. Fluorescence as a means of colour signal enhancement. *Philos. Trans. R. Soc. B.* **372**, 20160335 (2017).
26. Haddock, S. H. D. & Dunn, C. W. Fluorescent proteins function as a prey attractant: experimental evidence from the hydromedusa *Olindias oldi* and other marine organisms. *Biol. Open.* **4**, 1094–1104 (2015).
27. T. W. Cronin, S. Johnsen, N. J. Marshall, E. J. Warrant, *Visual Ecology*. (Princeton University Press, Princeton, NJ, 2014).
28. Endler, J. A. The color of light in forests and its implications. *Ecol. Monogr.* **63**, 2–27 (1993).
29. Anderson, S. R. & Wiens, J. J. Out of the dark: 350 million years of conservatism and evolution in diel activity patterns in vertebrates. *Evolution* **71**, 1944–1959 (2017).
30. Buchanan, B. W. Observed and potential effects of artificial night lighting on anuran amphibians. Ecological consequences of artificial night lighting, (eds Rich, C. & Longcore, T.) 192–220 (Washington, D.C., Island Press, 2006).
31. Fuller, R. C. Lighting environment predicts the relative abundance of male colour morphs in bluefin killifish (*Lucania goodei*) populations. *Proc. R. Soc. Lond. Ser. B: Biol. Sci.* **269**, 1457–1465 (2002).
32. Yovanovich, C. A. M. et al. The dual rod system of amphibians supports colour discrimination at the absolute visual threshold. *Philos. Trans. R. Soc. B: Biol. Sci.* **372**, 20160066 (2017).
33. Denton, E. J. & Wyllie, J. H. Study of the photosensitive pigments in the pink and green rods of the frog. *J. Physiol.* **127**, 81–89 (1955).
34. Robertson, J. M., Bell, R. C. & Loew, E. R. Vision in dim light and the evolution of color pattern in a crepuscular/nocturnal frog. *Evolut. Ecol.* **36**, 355–371 (2022).
35. Augusto-Alves, G., Dena, S. A. & Toledo, L. F. Visual communication and aggressive behaviour in a giant mute torrent-frog, *Megaelosia apuana* (Anura; Hylodidae). *Amphib.-Reptilia* **39**, 260–264 (2018).
36. Augusto-Alves, G. & Toledo, L. F. Communication across multiple sensory modes: quantifying the rich behavioural repertoire of a Neotropical torrent frog. *Behaviour* **159**, 351–375 (2021).
37. Brunner, R. M. & Guayasamin, J. M. Nocturnal visual displays and call description of the cascade specialist glassfrog *Sachatamia orejuela*. *Behaviour* **157**, 1257–1268 (2020).
38. Furtado, R., Lermen, L. N., Márquez, R. & Hartz, S. M. Neotropical dancing frog: the rich repertoire of visual displays in a hylodine species. *J. Ethol.* **37**, 291–300 (2019).
39. Hodl, W. & Amézquita, A. “Visual signaling in anuran amphibians” in *Anuran Communication* (Smithsonian Inst. Press, Washington). 121–141, 2001
40. de Sá, F. P., Zina, J. & Haddad, C. F. B. Sophisticated communication in the brazilian torrent frog *Hylodes japi*. *PLOS ONE* **11**, e0145444 (2016).
41. Mazel, C. H., Cronin, T. W., Caldwell, R. L. & Marshall, N. J. Fluorescent enhancement of signaling in amantiss shrimp. *Science* **303**, 51 (2004).
42. C. Kenneth Dodd Jr. *Frogs of the United States and Canada*. (John Hopkins University Press, Baltimore, MD, 2013).
43. S. Kumar, et al. TimeTree 5: An Expanded Resource for Species Divergence Times. *Molecular Biology and Evolution*, <https://doi.org/10.1093/molbev/msac174> (2022).
44. Kranz, A. M., Forgan, L. G., Cole, G. L. & Endler, J. A. Light environment change induces differential expression of guppy opsins in a multi-generational evolution experiment. *Evolution* **72**, 1656–1676 (2018).
45. Thomas, K. N. et al. Ecology drives patterns of spectral transmission in the ocular lenses of frogs and salamanders. *Funct. Ecol.* **36**, 850–864 (2022).
46. Wan, Y. et al. Selection on visual opsin genes in diurnal Neotropical frogs and loss of the SWS2 opsin in poison frogs (p. 2022.10.18.510514). *bioRxiv*. <https://doi.org/10.1101/2022.10.18.510514> (2023).
47. Aphalo, P. J. The r4photobiology suite: spectral irradiance. *UV4Plants Bulletin*. 21–29 <https://doi.org/10.19232/uv4pb.2015.1.14> (Helsinki, Finland, 2015).
48. Solar Spectra. Retrieved November 19, 2023, from <https://www.nrel.gov/grid/solar-resource/spectra.html>
49. Revell, L. “phytools 2.0: an updated R ecosystem for phylogenetic comparative methods (and other things).”. *PeerJ* **12**, e16505 (2024).
50. Höhna, L., Heath, B., Lartillot, M. & Huelsenbeck, R. RevBayes: Bayesian phylogenetic inference using graphical models and an interactive model-specification language. *Syst. Biol.* **65**, 726–736 (2016).

Acknowledgements

We would like to thank everyone who made this work possible, including all field stations at which data collection took place: Yasuni Scientific Station, El Amargal Nature Reserve, Los Amigos Conservation Hub (CIRCA), Fazenda Michelin, Estação Biológica Augusto Ruschi, Reserva Michelin, and Tartarugas da Amazonia (and surrounding indigenous communities including the Nova Esperança community of the Baré ethnic group and the Saracá community). Additionally, we thank Rafael Benettii, Lucas Neves, Victor Araújo, Thalia Corahua, and Schyler

Ellsworth for their help in the field and with sample preparation. We would like to thank Carlos Taboada for his advice on appropriate equipment and methodology during field expedition planning. Finally, we would like to thank our funding sources for making this work possible: The Lamarr and Edith Trott Scholarship (C.W.); The Explorers Club Rolex Grant (C.W.); Horace Loftin Endowment (C.W.); Martin Family Graduate Fellowship in Biological Sciences (C.W.); Society for Systematic Biologists Graduate Student Research Award (C.W.); Robert B. Short Scholarship in Zoology (C.W.).

Author contributions

Conceptualization: C.W., S.R.R., F.A.V., R.M.B. Methodology: C.W., S.R.R., F.A.V., A.C., V.H.A., E.C.U., F.G., R.M.B., A.L. Investigation: C.W., S.R.R., F.A.V., R.M.B. Visualization: C.W., A.L. Supervision: E.M.L. Writing—original draft: C.W. Writing—review & editing: C.W., S.R.R., F.A.V., A.C., V.H.A., E.C.U., F.G., R.M.B., A.L., E.M.L.

Competing interests

The authors declare no competing interests.

Additional information

Supplementary information The online version contains supplementary material available at <https://doi.org/10.1038/s41467-024-53111-w>.

Correspondence and requests for materials should be addressed to Courtney Whitcher.

Peer review information *Nature Communications* thanks the anonymous reviewers for their contribution to the peer review of this work. A peer review file is available.

Reprints and permissions information is available at <http://www.nature.com/reprints>

Publisher's note Springer Nature remains neutral with regard to jurisdictional claims in published maps and institutional affiliations.

Open Access This article is licensed under a Creative Commons Attribution-NonCommercial-NoDerivatives 4.0 International License, which permits any non-commercial use, sharing, distribution and reproduction in any medium or format, as long as you give appropriate credit to the original author(s) and the source, provide a link to the Creative Commons licence, and indicate if you modified the licensed material. You do not have permission under this licence to share adapted material derived from this article or parts of it. The images or other third party material in this article are included in the article's Creative Commons licence, unless indicated otherwise in a credit line to the material. If material is not included in the article's Creative Commons licence and your intended use is not permitted by statutory regulation or exceeds the permitted use, you will need to obtain permission directly from the copyright holder. To view a copy of this licence, visit <http://creativecommons.org/licenses/by-nc-nd/4.0/>.

© The Author(s) 2024